# THE EARTHQUAKE PREDICTION EXPERIMENT AT PARKFIELD, CALIFORNIA

Evelyn Roeloffs
*U.S. Geological Survey, Vancouver, Washington*

John Langbein
*U.S. Geological Survey, Menlo Park, California*

**Abstract.** Since 1985, a focused earthquake prediction experiment has been in progress along the San Andreas fault near the town of Parkfield in central California. Parkfield has experienced six moderate earthquakes since 1857 at average intervals of 22 years, the most recent a magnitude 6 event in 1966. The probability of another moderate earthquake soon appears high, but studies assigning it a 95% chance of occurring before 1993 now appear to have been oversimplified. The identification of a Parkfield fault "segment" was initially based on geometric features in the surface trace of the San Andreas fault, but more recent microearthquake studies have demonstrated that those features do not extend to seismogenic depths. On the other hand, geodetic measurements are consistent with the existence of a "locked" patch on the fault beneath Parkfield that has presently accumulated a slip deficit equal to the slip in the 1966 earthquake. A magnitude 4.7 earthquake in October 1992 brought the Parkfield experiment to its highest level of alert, with a 72-hour public warning that there was a 37% chance of a magnitude 6 event. However, this warning proved to be a false alarm. Most data collected at Parkfield indicate that strain is accumulating at a constant rate on this part of the San Andreas fault, but some interesting departures from this behavior have been recorded. Here we outline the scientific arguments bearing on when the next Parkfield earthquake is likely to occur and summarize geophysical observations to date.

## INTRODUCTION

Earthquake prediction research seemed on the verge of a breakthrough in 1975, when Chinese seismologists successfully alerted Haicheng city of an impending magnitude 7.3 earthquake [*Deng et al.*, 1981]. Public warnings were also achieved before the 1976 Songpan-Pingwu, China, earthquakes [*Wallace and Teng*, 1980] and the 1978 Izu-Oshima, Japan, earthquake (N. Nishide, oral communication, 1992). However, these early successes have not been repeated. Many seismologists even doubt the existence of measurable phenomena preceding earthquakes that might justify short-term predictions. Nonetheless, the search for earthquake precursors continues worldwide, much of it in focused earthquake prediction study areas in Japan, Turkey, the former Soviet Union, and China. In the United States a focused earthquake prediction study is in progress at Parkfield, California.

The town of Parkfield, built practically on the San Andreas fault about halfway between San Francisco and Los Angeles (Figure 1), experienced moderate earthquakes in 1857, 1881, 1901, 1922, 1934, and, most recently, a magnitude 6 event in 1966. On the basis of this sequence of events, *Bakun and Lindh* [1985] estimated the recurrence interval for magnitude 6 earthquakes near Parkfield as 22 ± 3 years and conjectured with 95% confidence that another such event would occur before 1993. The Parkfield Earthquake Prediction Experiment began in 1985, after Bakun and Lindh's conjecture was accepted by the National Earthquake Prediction Evaluation Council (NEPEC) and the California Earthquake Prediction Evaluation Council (CEPEC) [*Shearer*, 1985*a*, *b*]. One million dollars of initial funding for instrumentation was provided by the U.S. Geological Survey (USGS) and was matched by the state of California. The experimental goals are to record geophysical signals accompanying the earthquake process at Parkfield, to capture effects of strong motion in the near field, and, most ambitiously, to attempt to issue a warning up to 3 days before the magnitude 6 event if seismicity and/or fault creep rate reach predefined threshold levels.

Eight years into the experiment, 21 instrument networks designed to record preearthquake phenomena operate near Parkfield (Tables 1*a* and 1*b*) [*Bakun*, 1988*b*], five of which are monitored in real time. Ten more networks wait to record strong motion, coseismic slip, and liquefaction (Table 1*c*) [*Sherburne*, 1988] when a moderate earthquake occurs. Investigators from 13 institutions in addition to the USGS participate. Including a seismic network that records and locates all events above magnitude 1.0, the instrumentation at Parkfield is unmatched in diversity and density by that of any other earthquake prediction study worldwide.



Reviews of Geophysics, 32, 3 / *August 1994*
pages 315–336
Paper number 94RG01114

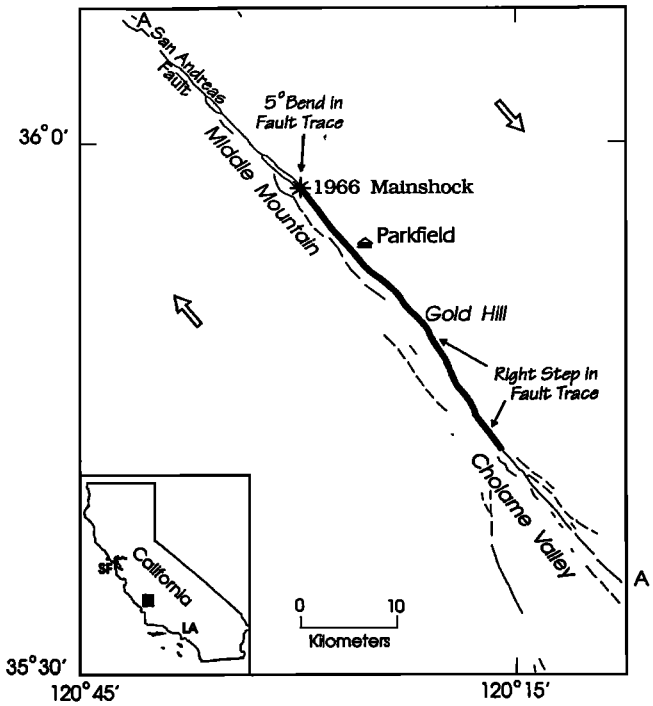


**Figure 1.** Parkfield experiment landmarks along the San Andreas fault in central California. In the inset California map the solid rectangle is the location of map area; SF denotes San Francisco; LA denotes Los Angeles. Arrows indicate the direction of motion of the Pacific plate relative to the North American plate. The San Andreas fault is darkened over the approximate extent of surface rupture associated with the 1966 Parkfield earthquake as mapped by *Brown* [1970].

Since the initial two-million-dollar startup funding, virtually all work at Parkfield has been carried out within the previously existing budget of the National Earthquake Hazards Reduction Program (NEHRP). In this sense, the Parkfield experiment constitutes a commitment to concentrate monitoring instruments in a single area with a high probability of experiencing an earthquake soon. Such a concentration is desirable because reports of earthquake precursors will be more credible if they are corroborated by signals on other instruments and because long baselines of data may be necessary in order to determine whether small pre-earthquake signals are anomalous.

A unique and important feature of the Parkfield experiment, which enabled it to receive start-up funds from California, is its prototypical plan for communicating earthquake hazard information to the California Office of Emergency Services (OES). *Bakun et al.* [1986, 1987] and *Bakun* [1988*c*] describe the plan in detail. "Alert/status" thresholds have been defined for six instrumentation networks (Table 1a). The seismic and creep thresholds reflect phenomena preceding the 1966 Parkfield earthquake, but such data are not available for the other instruments. Instead, their thresholds are set so that, statistically, signals unusual enough to meet them occur with specified frequency. When a signal exceeds a threshold (usually detected by a computer program that can page a scientist), scientists monitoring all six of these networks are notified. There are five alert/status levels, with notification to OES at all but the two lowest levels. At the highest level (level A) the notification to OES states that there is a 37% chance that the magnitude 6 Parkfield earthquake will happen within the next 72 hours. Before the Parkfield plan was fully exercised, response plans for volcanic unrest at Long Valley Caldera [*Hill et al.*, 1991] and for earthquake hazard in southern California [*Jones et al.*, 1991] had already been modeled after it.

The NEPEC- and CEPEC-sanctioned prediction window for Parkfield officially closed on December 31, 1992, but the predicted magnitude 6 earthquake did not occur. Focused study of Parkfield has generated controversy over the simple picture of cyclically recurring seismicity that motivated the experiment. During the interval of the experiment, California suffered two magnitude 7 earthquakes near major population centers that are less well instrumented than Parkfield. Many have expressed concern that concentration of earthquake prediction resources at Parkfield may be a

**TABLE 1a. Prediction Monitoring Networks at Parkfield With Defined Alert/Status Levels as of November 1992**

| *Network* | *Number of Sites* | *Sensitivity/ Threshold* | *Measurement Interval* | *References* |
|---|---|---|---|---|
| Seismicity (USGS Calnet) | 40 | Magnitude 1.0 | continuous | *Nishioka and Michael* [1990] |
| Continuous strain* | 6 | $10^{-9}$ | 10 min | *Myren and Johnston* [1989] |
| Magnetic field | 7 | 0.25 nT | 10 min | *Mueller et al.* [1994] |
| Creep meters (Invar wire-LVDT†) | 13 | 0.01 mm | 10 min | *Schulz* [1989] |
| Groundwater level* | 10 | 1 mm | 15 min | *Roeloffs et al.* [1989] |
| Two-color laser geodimeter | 18 lines | 1 mm | 3 times/week | *Langbein et al.* [1990] |

All of these networks are operated by USGS, Menlo Park, California. Reference describes network and/or measurement technique.

*The sensitivity in the table is appropriate for signals with durations of 24 hours or less. Because of increasing Earth noise at longer periods, signals must be larger to be detected at longer periods (see, for example, *Langbein et al.* [1993]).

†LVDT, linear variable differential transformer.

**TABLE 1b. Prediction-Oriented Networks at Parkfield Without Alert/Status Levels as of November 1992**

| *Network and Operator* | *Number of Sites* | *Sensitivity/ Threshold* | *Measurement Interval* | *References* |
|---|---|---|---|---|
| Borehole tensor strain;*† University of Queensland, Australia | 2 | $10^{-9}$ | 10 min | *Gladwin et al.* [1987] |
| Tilt;*† USGS | 5 | 1 μrad | 10 min | *Mortensen et al.* [1978] |
| Groundwater radon;[2] USGS | 2 | 1 pCi/L | 10 min | *Noguchi and Wakita* [1977] |
| Soil hydrogen;[2] USGS, Reston | 7 | 10 ppm | 10 min | *Sato et al.* [1986] |
| Borehole microtemperature; USGS | 1 | $10^{-4}$ °C | 12 min | C. Williams (oral communication, 1992) |
| Resistivity; UC, Riverside | 6 dipoles | 1% | daily average | *Park* [1991] |
| 80-kHz magnetic field; University of Alaska | 1 | 0.5 μV | 6 s | E. Wescott (oral communication, 1992) |
| 0.01- to 10-Hz magnetic field; Stanford University | 2 | 1 pT | 30 min, average | *McGill et al.* [1993], *Bernardi et al.* [1991] |
| Trilateration (4 to 33 km lines); USGS | 113 lines | 3 mm + 0.2 mm/km | yearly | *King et al.* [1987] |
| Small-aperture nets (3 to 4 km lines); USGS | 4 | 3–4 mm | yearly | *King et al.* [1987] |
| GPS; USGS, SIO | 4 | <1 cm north, east; 1–2 cm vertical | 4 times per year | *Prescott et al.* [1989] |
| Rapid static GPS; JPL, USGS | 107 | 2 mm | yearly | *Hurst et al.* [1992] |
| Continuous GPS; SIO, JPL, USGS | 1 | 1 cm | continuous | K. Hudnut (oral communication, 1992) |
| Highway 46 GPS array; USGS, SIO | 16 | 1 cm | 2 times per year | K. Hudnut (oral communication, 1992) |
| Leveling; UC, Santa Barbara | 7 lines | 1 mm/km | yearly | *Sylvester* [1991] |
| Creep meters (Invar rod-digital caliper); CIRES | 3 | 0.2 mm | 1 min | J. Behr and R. Bilham (oral communication, 1992) |
| Acoustic emission (30, 60, 170 kHz); IBM, USGS | 1 | 1 μbar | continuous | *Armstrong and Valdes* [1991] |
| Borehole seismometers; Duke University, LBL, UCB | 10 | magnitude 0 | continuous | *Michelini et al.* [1991] |
| Vibroseis waveform; LBL, UCB | 80 paths, 9 components | 5 ms | 4–5 times per year | *Karageorgi et al.* [1992] |
| Vertical seismic array; LBL, UCB, Duke University | 1 | 32 three-component to 1000 m | continuous | *Daley et al.* [1990] |
| GPS; SIO | 2 lines | <1 cm north, east; 1 cm vertical | 1–2 times per year | Y. Bock (oral communication, 1992) |

Abbreviations are CIRES, Cooperative Institute for Research in Environmental Sciences; GPS, Global Positioning System; JPL, Jet Propulsion Laboratory, California Institute of Technology; LBL, Lawrence Berkeley Laboratories; SIO, Scripps Institution of Oceanography, University of California, San Diego; UC, University of California; UCB, University of California, Berkeley; and USGS, U.S. Geological Survey.

*The data in the table are appropriate for signals with durations of 24 hours or less. Because of increasing Earth noise at longer periods, signals must be larger to be detected at longer periods (see, for example, *Langbein et al.* [1993]).

†Data from these networks are sent via GOES satellite to Menlo Park, California, using the system described by *Silverman et al.* [1989].

poor strategy. *Michael and Langbein* [1993] summarize a meeting of Parkfield investigators convened to evaluate the experiment near the close of the prediction window.

Here we review current thinking about when the next Parkfield earthquake might occur, and we summarize research results obtained so far using data collected at Parkfield. We have chosen not to emphasize our own opinions; instead, we hope this article will facilitate informed debate on earthquake prediction research strategy.

## GLOSSARY

Further information on many of these terms is given by *Aki and Richards* [1980].

**Aseismic:** without the occurrence of an earthquake.

**Asperity:** part of a fault plane that tends to rupture in earthquakes, generally believed to have greater resistance to failure than surrounding parts of the fault plane that slip aseismically.

***b* value:** for a particular region and time interval the best fitting coefficient $b$ in the relationship $\log_{10}$

**TABLE 1c. Instrumentation Designed to Record Rupture Propagation and/or Strong Ground Motion for Engineering Applications**

| *Network and Operator* | *Number of Sites or Instruments* | *References* |
|---|---|---|
| Dense seismic array; USGS | 14 geophones, 14 accelerometers in a 1 $km^2$ area | *Fletcher et al.* [1992] |
| Liquefaction array; EPRI, USGS | 5 accelerometers, 7 piezometers, vertical benchmarks | *Holzer et al.* [1988] |
| EPRI dense accelerograph array; EPRI, CDMG | 21 three-component FBA (13 surface, 8 subsurface) within a 120-m radius | *Schneider et al.* [1990] |
| CDMG strong motion array; CDMG | 48 three-component SMA | *McJunkin and Shakal* [1983] |
| GEOS digital recording (acceleration, velocity, volumetric strain); USGS | 13 three-component FBA, 7 geophones, 6 borehole strain meters | *Borcherdt et al.* [1985, 1988] |
| Fault rupture video camera; USGS | 2 cameras | |
| Coseismic slip meter; CalTech | 1 | K. Hudnut (oral communication, 1992) |
| Pipeline experiment; Weidlinger Associates | 2 strain-gaged pipeline segments, 8 ductile iron pipes | *Isenberg et al.* [1989, 1991] |
| Turkey flat strong-motion array; CDMG | six three-component FBA (four surface, two downhole), 2-km linear array | *Real and Tucker* [1988] |

Abbreviations are CalTech, California Institute of Technology; CDMG, California Division of Mines and Geology; EPRI, Electric Power Research Institute; FBA, force-balance accelerometer; and USGS, U.S. Geological Survey.

$N = a - b\,M$, where $N$ is total number of earthquakes magnitude $M$ or larger; $b$ is usually near 1.

**Borehole strain meter:** Borehole volumetric strain meters (also called "dilatometers") are described by *Sacks et al.* [1971]. Borehole tensor strain meters, which measure deformation along three horizontal axes, are described by *Gladwin et al.* [1987].

**Coda Q:** The coda is the final part of a seismogram, which typically decays with a regular envelope. The rate of decay can be quantified by a quality factor, $Q$, with higher values of $Q$ representing slower decay. It has been proposed that coda $Q$ changes before some earthquakes, possibly caused by changes in the physical state of the earthquake nucleation volume.

**Coseismic:** occurring at the time of (but not preceding) an earthquake.

**Epicenter:** point on the Earth's surface directly above an earthquake hypocenter.

**Fault creep:** fault slip that takes place aseismically (without earthquakes).

**Hypocenter:** location in three dimensions of an earthquake or (for a large earthquake) its nucleation point.

**Interseismic:** occurring in the period between earthquakes.

**Invert:** to estimate the parameters of a function using observational data.

**Moment:** a measure of the size of a seismic or aseismic slip event on part of a fault plane. The moment is the product of slip, area, and shear modulus. The shear modulus is often thought of as a constant. The product of slip and area is frequently more easily inferred than either of those quantities individually.

**Nucleation:** the initiation of an incipient earthquake rupture.

**Quiescence:** a decrease in the rate of background seismicity.

**Retime:** redo the process of reading arrival times from seismograms in order to improve on previous readings, especially when the previous readings were made by a computer program.

**Seismogenic:** capable of producing an earthquake, usually referring to a fault or a part of a fault.

**Shear wave splitting:** progressive separation of orthogonally polarized shear wave fronts as a wave train propagates through a medium with anisotropic shear wave velocity.

**Velocity inversion:** determination of three-dimensional seismic velocity structure by solving simultaneously for earthquake source locations and velocity variations along source-receiver paths.

**Wood-Anderson seismograph:** a standard seismograph in use since the early 1900s, records from which were used to define the original Richter magnitude

scale. Wood-Anderson stations that still operate provide seismograms that can be compared with those recorded decades ago on the same instrument.

## SCIENTIFIC RATIONALE FOR PREDICTION MONITORING AT PARKFIELD

As nearly as can be determined from available recordings, magnitude 6 Parkfield earthquakes in 1934 and 1966 nucleated in exactly the same location beneath Middle Mountain (Figure 1), and the 1922 Parkfield earthquake is known to have occurred within 18 km to the northwest of that epicenter [*Bakun*, 1988*a*]. The design of prediction monitoring experiments at Parkfield is tailored to the assumption that the next magnitude 6 earthquake will also occur beneath Middle Mountain.

Even more remarkable than the closely spaced mainshock locations is that both the 1934 and 1966 events had foreshocks that preceded the respective mainshocks by 17 min and that Wood-Anderson seismograms for these foreshocks are strikingly similar [*Bakun and McEvilly*, 1979], suggesting a common nucleation point. In 1934 there were also earlier foreshocks, including a magnitude 5 event 55 hours before the mainshock [*Bakun and McEvilly*, 1981]. The history of foreshocks suggests that it is reasonable to expect a foreshock before the next magnitude 6 event as well. In the Parkfield alert/status scheme, earthquakes within about 5 km of the 1966 hypocenter lead to higher alert levels than those within the general Parkfield area; a single event of magnitude 4.5 or greater there is considered a potential foreshock and brings the experiment to an A level alert.

Although its public policy impact would be significant, a public warning of a magnitude 6 Parkfield event based on foreshocks alone would not be a scientific breakthrough, since it has already been established that foreshocks precede about 35% of southern California earthquakes of magnitude 5 or larger [*Jones*, 1984]. The more controversial issue is whether other types of earthquake precursors take place. Two anecdotes suggest that accelerated but aseismic fault slip preceded the 1966 Parkfield earthquake [*Allen and Smith*, 1966]. Twelve days before that event a group of visiting Japanese seismologists noticed a set of fresh-appearing en-echelon cracks in the surface trace of the San Andreas fault about 2 km south of Parkfield. According to *Smith and Wyss* [1968], the ground cracking was taken seriously enough that a portable seismograph was deployed at that location for 24 hours 3 days later. Nine hours before the magnitude 6 earthquake, an irrigation pipe crossing the fault trace about halfway between Parkfield and Gold Hill ruptured. If these observations are attributable to aseismic fault slip, and if such slip also precedes the next earthquake in Parkfield, then it should be detected by the Parkfield creep meter network.

Seismologists in China and the former Soviet Union commonly cite earthquake precursors that take place as far as a few hundred kilometers from the impending epicenter. In contrast, the Parkfield experimental design philosophy is that precursors are most likely to be recorded close to the epicenter. This notion is consistent with the state- and rate-dependent friction laws recently developed from laboratory studies [*Dieterich*, 1979*a*, *b*; *Ruina*, 1983; *Blanpied et al.*, 1987]. If these laws are relevant to the seismic failure of natural faults, it seems likely that aseismic fault slip near the hypocenter may precede the nucleation of an earthquake rupture. If enough such slip occurs, it would produce near-surface deformation that might be detectable. For this reason, several instrumentation networks in Parkfield measure crustal deformation directly. Other networks measure quantities such as groundwater level, resistivity, and magnetic field variations that can change in proportion to crustal deformation.

A significant amount of aseismic slip at the hypocenter of the 1966 earthquake could elude detection by even the most sensitive crustal deformation instruments, such as borehole strain meters. When a magnitude 4.7 earthquake took place in October 1992, its static strain field produced coseismic steps of 20 nanostrain or less on borehole strain meters located in the northern half of the Parkfield rupture zone. No other instrument was sensitive enough to record low-frequency strain associated with this earthquake, which represented about 20 cm of slip over a square kilometer of fault plane at 10 km depth [*Parkfield Working Group*, 1993]. If this slip had occurred over a period of 2–3 days rather than seconds, it would not have been detectable in the borehole strain records because their noise level increases as periods lengthen [*Langbein et al.*, 1993]. It seems plausible that slip preceding an earthquake should have moment less than that of the earthquake itself. In fact, borehole strain measurements before five moderate earthquakes detected no preearthquake strain, demonstrating that in those cases, preseismic slip either did not occur or had moment less than a few percent of the earthquake moment [*Johnston et al.*, 1987].

Since direct measurement of the strain associated with postulated preseismic slip may be impossible with existing instrumentation, other experiments at Parkfield are monitored because they may have recorded anomalous preseismic phenomena in other places. One example is the ultralow frequency (0.01 Hz to 32 kHz) magnetic field monitoring system, which duplicates instrumentation that recorded magnetic field disturbances prior to the 1989 Loma Prieta earthquake [*Fraser-Smith et al.*, 1990; *McGill et al.*, 1993]. Geochemical monitoring has a similar motivation.

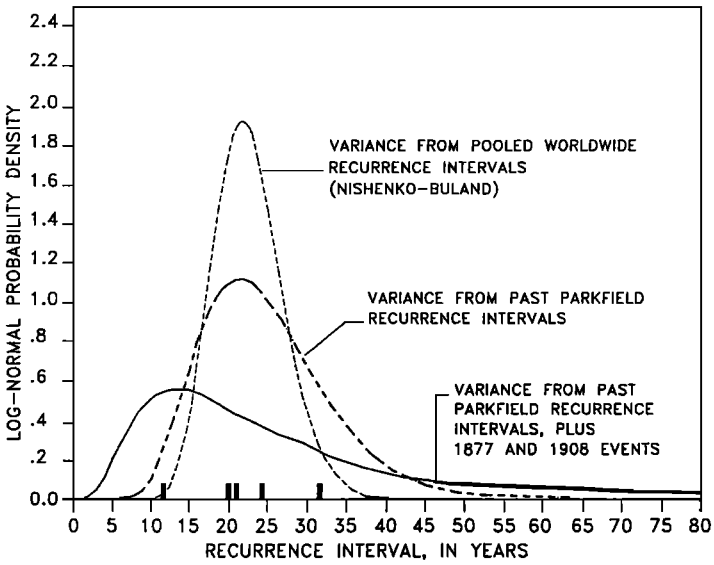


**Figure 2.** Lognormal probability density functions that might govern the distribution of earthquake recurrence intervals at Parkfield, California. The dashed curve labeled "Nishenko-Buland" has a mean recurrence interval of 21 years and a shape factor of 0.21; the dot-dashed curve with variance computed from Parkfield earthquake dates has the same mean recurrence interval but a shape factor of 0.35. The solid bars on the horizontal axis denote recurrence intervals from the historical record of earthquakes in Parkfield in 1857, 1881, 1901, 1922, 1934, and 1966. Other Parkfield events may have occurred in 1877 and in 1908; including these events yields an estimate of 12.9 years for the mean recurrence interval and a value of 0.70 for the shape factor (solid curve).

## THE STATISTICAL DISTRIBUTION OF PARKFIELD INTEREVENT INTERVALS

*Bakun and Lindh* [1985] listed 1857, 1881, 1901, 1922, 1934, and 1966 as the dates of past Parkfield earthquakes. The mean recurrence interval of these events is 22 years, with a standard deviation of 7.2 years. The first three recurrence intervals are closely clustered, and if the 1934 earthquake had occurred in 1944 instead, then all five recurrence intervals would be nearly identical. *Bakun and Lindh* [1985] postulated a Parkfield recurrence model in which a characteristic earthquake must occur once a critical level of fault stress is reached but in which an occasional early failure might be triggered. Treating the 1934 event as an early failure, they fit a straight line to the dates of the other Parkfield earthquakes as a function of earthquake sequence number and concluded, with 95% confidence that the time of the next event should be 1988 ± 5 years. This confidence estimate is based on the tacit assumption that Parkfield earthquake recurrence intervals are normally distributed and, as Bakun and Lindh themselves noted, is of limited meaningfulness. A basic problem is that five interevent intervals are not enough to define a statistical distribution.

Recognizing that no single fault segment has experienced enough characteristic earthquakes (see next section) to define the statistical distribution of the recurrence intervals, *Nishenko and Buland* [1987] pooled data from sequences of characteristic earthquakes in many geographic regions to arrive at a "generic" distribution of recurrence intervals. In order to pool recurrence intervals for different faults they normalized the data by determining an average recurrence interval for each segment, $T_{ave}$, and evaluated the distribution of $T/T_{ave}$ for all the recurrence intervals $T$ known for all segments. They fit these data to a lognormal distribution, in which the natural logarithms of the pooled recurrence intervals are normally distributed. The lognormal distribution, unlike the more fundamental Gaussian distribution, is limited to positive values of the recurrence interval and skewed toward longer recurrence intervals, as are the observations. Nishenko and Buland showed that a fairly good fit to the pooled normalized recurrence intervals is obtained with a lognormal distribution having a "shape factor" of 0.21 (Figure 2). The shape factor is the standard deviation of the logarithms of the normalized recurrence intervals, so a shape factor of 0.21 says essentially that recurrence intervals within one standard deviation of the mean range from 81% to 123% of the average recurrence interval. Using this distribution, *Nishenko and Buland* [1987] computed the expected time of the next Parkfield earthquake as 1987, with a 90% confidence level window of 8.2 years. Clearly, Nishenko and Buland assign a lower probability of having the earthquake before 1993 than did *Bakun and Lindh* [1985]. The reason for the difference is that by omitting the 12- and 32-year recurrence intervals from their calculations, Bakun and Lindh implicitly arrived at a narrower distribution than did Nishenko and Buland.

*Savage* [1991] questioned whether the shape factor of 0.21 is really consistent with the Parkfield recurrence intervals. He compared the Parkfield recurrence intervals with artificial sequences of recurrence intervals generated from a lognormal distribution having a shape factor of 0.21. Only 2% of the sequences he generated fit the Nishenko-Buland distribution as poorly as the observations; i.e., the observed sequence of Parkfield recurrence intervals is inconsistent with the Nishenko-Buland distribution at the 98% confidence level. Savage then fit the Parkfield recurrence intervals themselves to a lognormal distribution; he

obtained a shape factor of 0.35 and a mean recurrence interval of 21 years (Figure 2). The Nishenko-Buland distribution yields a conditional probability of 30% that the next Parkfield earthquake will occur before 1995, given that it had not yet happened as of October 1993 (27.3 years after the last event). If the shape factor of 0.35 estimated directly from the Parkfield recurrence intervals is used, the corresponding conditional probability is 15%, with about a 45% chance the event will take place before 1998. *Savage* [1993] further points out that a reevaluation of *Bakun and Lindh*'s [1985] probability is in order, because the failure of the next Parkfield earthquake to occur before the beginning of 1992 is inconsistent with their hypothesis at the 95% confidence level.

Clearly, there is considerable disagreement about the probability of the next Parkfield earthquake, even if it can be assumed that the six dates listed by *Bakun and Lindh* [1985] are the correct ones to use. However, there are no instrumental records of earthquakes in central California before 1898. *Toppozada* [1992], by investigating historical sources, has identified several previously unknown events of magnitude greater than 5.25 within 100 km of Parkfield before 1930; two of these, in 1877 and 1908, appear to have been on the San Andreas fault. If these smaller earthquakes were included in the set used to fit a lognormal distribution, then the mean recurrence time is 12.9 years and the shape factor is 0.70 (Figure 2). In this case, the conditional probability of having the next Parkfield earthquake before 1995, given that it had not yet happened 27.3 years after the last event, is only 9%.

*Davis et al.* [1989] showed that when the recurrence interval distribution is "updated" to include the present period of repose, the estimated probability of a magnitude 6 earthquake in the next year decreases as time passes without such an event. This paradoxical result, which arises because the variance of the recurrence interval estimate increases as the current repose interval lengthens well past the mean of 22 years, conflicts with the physical situation of continually building strain.

The *Working Group on California Earthquake Probabilities* (*WGCEP*) [1988] noted that only for the central creeping segment of the San Andreas fault is there recurrence interval information as reliable as the record of six historical events at Parkfield. Applying the Nishenko-Buland distribution to the San Andreas fault system, they estimated the conditional probability of a magnitude six earthquake at Parkfield before 2018 as greater than 90%, the highest 30-year probability assigned to any segment of the San Andreas fault system. Although it is generally agreed that the probability given by Bakun and Lindh was unrealistically high, no location is known for which the probability of an imminent magnitude 6 earthquake is greater than at Parkfield.

## WHAT DEFINES THE PARKFIELD "SEGMENT"?

The technique of earthquake hazard forecast used by the WGCEP is based on the idea of fault segmentation, in which faults can be divided into "segments" such that each segment tends to rupture as a unit. These segments are often partly defined by geometric features in the surface fault trace. A further assumption, for which Parkfield has been presumed to be the classic example, is that most of the strain release on the segment occurs in repeated earthquakes of similar size, called "characteristic earthquakes." Once the rupture zone is assumed known and time-invariant, it is conceptually simple to forecast the time of the next earthquake based on the long-term strain accumulation rate and the slip observed in past characteristic events. However, detailed study at Parkfield has shown that geometric fault features visible on maps probably do not cause the unique behavior of the Parkfield segment.

Middle Mountain, the northwestern limit of the 1966 Parkfield rupture zone, was the nucleation site from which the main shock ruptured to the southeast, as well as the location of a foreshock that propagated northwest [*Bakun and McEvilly*, 1979]. Today, the rates of both shallow seismicity (Figure 3) and creep on the San Andreas fault decrease to the southeast of Middle Mountain. There is a 5° bend in the surface trace of the fault at Middle Mountain (Figure 1), and *Lindh and Boore* [1981] noticed that earthquakes located north and south of the bend have first-arrival motions of opposite polarity at a station near Gold Hill (Figure 1). They interpreted the polarity change as evidence that the bend extends to seismogenic depths and inferred that this bend controls the northern limit of the Parkfield fault segment. However, when *Nishioka and Michael* [1990] retimed and relocated seismicity from 1984 to 1987 near Middle Mountain, they found no bend in the plane defined by the hypocenters, although they confirmed the pattern of first-arrival polarities discovered by Lindh and Boore. Thus the contrasting seismicity northwest and southeast of Middle Mountain cannot be explained by the mechanical effects of the bend in the surface trace.

*Eaton et al.* [1970] noticed that aftershock hypocenters of the 1966 Parkfield earthquake apparently defined a surface with a bend just south of Gold Hill, near the point where the dynamic rupture seemed to have slowed down. The bend underlies a 1-km right step in the surface fault trace (Figure 1). Further evidence that this step helped arrest the dynamic rupture in 1966 was presented by *Lindh and Boore* [1981], who perceived a stopping phase originating near Gold Hill in strong motion records. Lindh and Boore argued that after passing the step, the main shock rupture continued southeast for another 5 s (1–2 km). On the other hand, in an independent analysis, *Archuleta and Day*

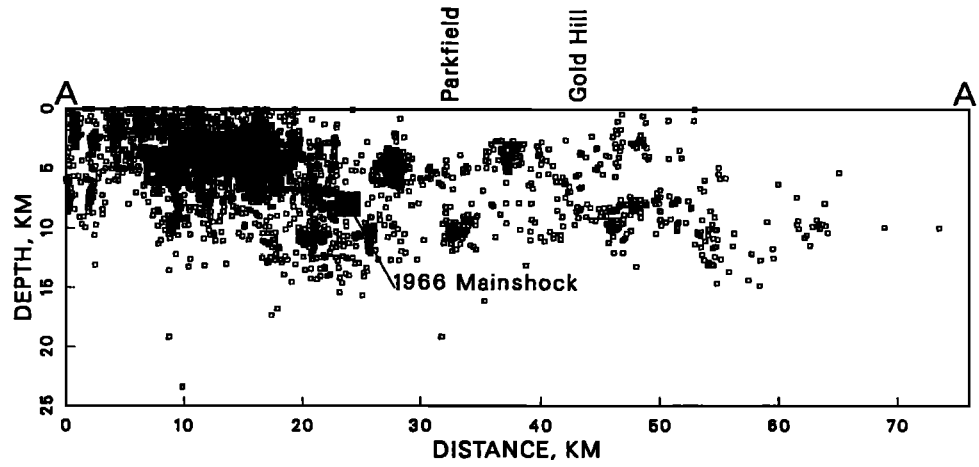


**Figure 3.** Vertical cross section looking northeast at the plane of the San Andreas fault near Parkfield showing background seismicity since 1969. Except for the 1966 mainshock, all events have magnitudes between 0.5 and 4.3 but are shown with the same size symbol. Locations of A and A′ are shown in Figure 1.

[1980] concluded that a rupture that propagated 5 km past the step fit the same data satisfactorily.

Although *Segall and Pollard* [1980] had shown that a right step should not impede a propagating right-lateral rupture, *Sibson* [1985] argued that pore fluid suction induced by the rupture front could be a barrier to dynamic slip. Postseismic surface slip southeast of the step could then be explained by the gradual relaxation of stress as pore pressure rose back to its previous value.

Interestingly, when the microseismicity recorded since 1983 is relocated using a three-dimensional velocity model, the step in the fault trace south of Gold Hill is not apparent [*Aviles and Michael*, 1990; *Eberhart-Phillips and Michael*, 1993] (Figure 4). *Michael and Eberhart-Phillips* [1991*b*] and *Eberhart-Phillips and Michael* [1993] used the same velocity model to relocate the aftershocks of the 1966 Parkfield earthquake and showed that the bend observed by *Eaton et al.* [1970] disappeared. The 1966 aftershocks apparently occurred on the same plane that is defined by the post-1983 background seismicity.

The Gold Hill exotic block [*Sims*, 1988, 1989, 1990] (Figure 4) is evidence that the San Andreas fault has straightened its active surface trace in the past, perhaps by rupturing through fault offsets. This block was formerly part of a larger fragment that originated about 160 km south of Gold Hill on the southwest side of the San Andreas fault and was transported northwest by right-lateral motion. The Gold Hill gabbro and associated sedimentary rocks were separated from the larger fragment and left northwest of the active fault trace when right-lateral motion was transferred to the present more southwesterly fault trace. The fossil trace of the San Andreas fault which formerly bounded the Gold Hill exotic block to the northeast is now visible as the Jack Ranch fault (Figure 4). Since the vertical plane extending downward from the creeping trace of the San Andreas fault southwest of Gold Hill is now without microseismicity, this portion of the fault trace may also be becoming inactive. Such a fault-straightening process would tend to remove the right step that may have helped arrest southeastward rupture in past Parkfield earthquakes.

There is in fact evidence that slip in 1966 extended further south than it did in 1934. *Savage and Burford* [1973] and *Segall and Du* [1993] showed that slip in 1934 stopped north of a triangulation net that crosses the fault near the right step, while in 1966, slip continued southeastward through the net, 10 km south of the right step. This slip may have been in the form of postseismic slip rather than dynamic rupture.

More evidence that the dilational jog is an actively evolving feature was presented by *Shedlock et al.* [1990], whose high-resolution reflection profiling suggested that the jog may be propagating southeastward, a plausible result of earthquakes that rupture through the right step.

Although it now appears that the superficial geometric features at the ends of the Parkfield rupture zone do not extend to depths where they might play a mechanical role in the earthquake process, newly discovered subsurface features near Middle Mountain and Gold Hill might indeed play such roles. Recently, *Michael and Eberhart-Phillips* [1991*a*] and *Eberhart-Phillips and Michael* [1993] have identified a body of relatively low compressional wave velocity ($V_p$) and low resistivity abutting the northeast side of the fault to a depth of 8 km beneath Middle Mountain, reaching to just above the 1966 hypocenter. They infer that pore fluid pressure is high within this body. Lateral refraction of seismic waves traversing this complicated area could explain the opposite first-arrival polarities at Gold Hill for earthquakes north and south of the 5° bend. Furthermore, most of the 1966 moment release occurred over 20 km of the fault trace adjoined by

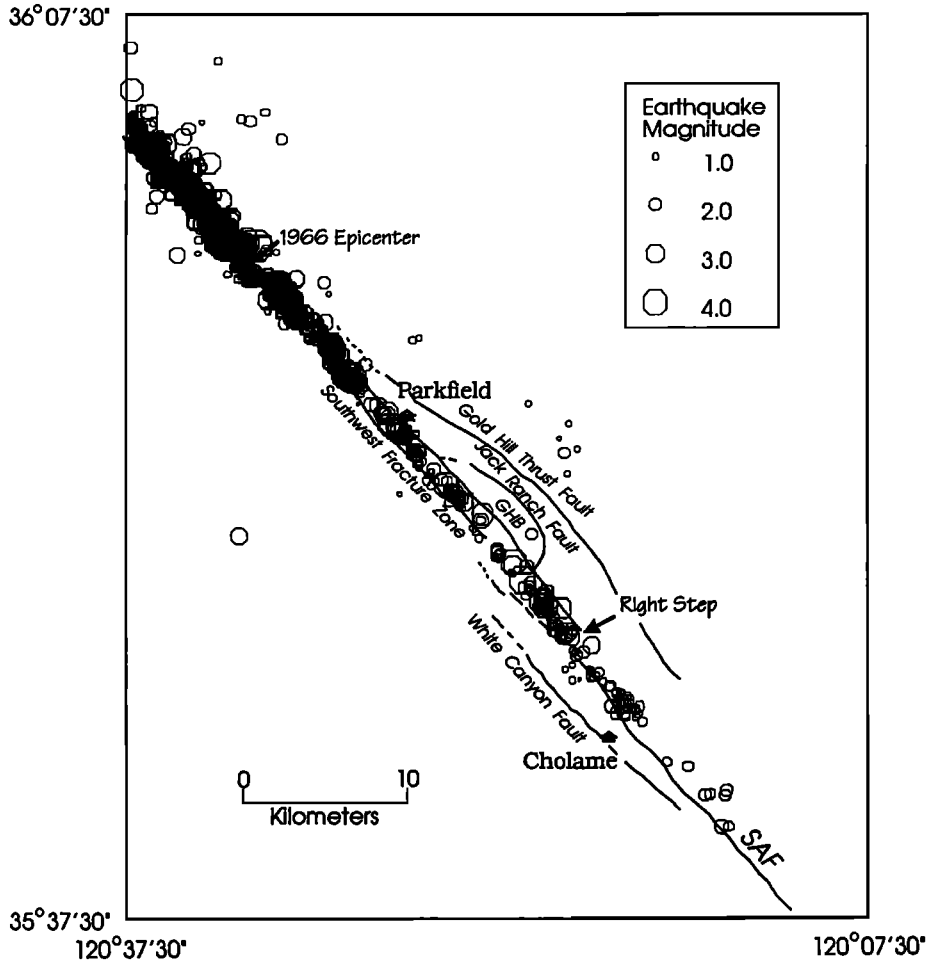


**Figure 4.** The San Andreas fault (SAF) near Parkfield, showing the right step originally proposed to have arrested rupture in the 1966 Parkfield earthquake. The Gold Hill and Jack Ranch faults and the Gold Hill exotic block (GHB) are shown from *Sims* [1990]. Symbols indicate epicenters of microearthquakes recorded between 1984 and 1990 and relocated with a three-dimensional velocity model [*Eberhart-Phillips and Michael*, 1992].

relatively high velocity material on the northeast side, near Gold Hill.

*Michelini and McEvilly* [1991] included recordings from the high-resolution network of borehole seismometers surrounding Middle Mountain in a three-dimensional (3-D) velocity inversion over a grid centered at the 1966 epicenter and extending 25 km along the fault trace to a depth of 10 km. They found low shear wave velocity ($V_s$) at depths of 5–9 km near the 1966 hypocenter and also showed that this volume has a relatively high $V_p/V_s$ of 2.0, possibly indicative of high pore pressure. Their inversion revealed that a pronounced low-velocity zone between depths of 3 and 9 km characterizes the creeping section of the San Andreas fault northwest of Middle Mountain but that this zone is not present along the fault stretch that ruptured in 1966.

Also using accurate locations of microearthquakes from the borehole seismometer network, *Malin et al.* [1989] identified two aseismic patches on the San Andreas fault plane north and south of Middle Mountain; they believe these patches will slip in the next magnitude 6 Parkfield event, that is, that the patches are parts of the Parkfield "asperity."

The Parkfield segment can still be thought of as the rupture zone of the 1966 Parkfield earthquake, and it behaves distinctively: near-plate-rate creep and steady background seismicity both taper to zero from its northwestern to its southeastern limit. However, detailed seismic, geologic, and geodetic work suggest that a 5° bend and a 1-km right step do not control this behavior. Instead, seismic imaging has revealed physical property variations at seismogenic depths near the segment ends. How these features could control rupture initiation and arrest remains to be investigated.

## STRAIN BUDGET ESTIMATES AND THE PARKFIELD PREDICTION

Geodetic measurements made near Parkfield allow estimation of the slip deficit accumulated since the 1966 earthquake, relative to the presumably continuous relative displacement across the North American–Pacific plate boundary at depth. *Segall and Harris* [1986, 1987] and *Harris and Segall* [1987] inverted repeated distance measurements made between 1966 and 1984 to determine the distribution of slip rate on the San Andreas fault during and since the 1966 Parkfield earthquake. These three papers, which will be referred to collectively as SH, indicate that there has been very little interseismic slip on the rupture zone of

the 1966 Parkfield earthquake and that the zone of little slip must extend almost as far north as the 1966 epicenter. *Snay* [1989] reached similar conclusions using an alternative analysis. On the basis of the moment of the 1966 earthquake and the slip deficit accumulation rate, SH concluded that a magnitude 6 earthquake near Parkfield was most likely between 1984 and 1989 but might not occur until 1995 (Figure 5).

Many slip distributions can fit the geodetic data. In particular, SH's analysis scheme required an assumed value for the "transition depth" between the deep, steadily creeping ductile part of the fault and the shallower seismogenic zone. SH found that depths between 14 and 22 km fit the data acceptably well, if the slip rates below that depth were chosen as 25 and 33 mm/yr, respectively (Figure 16 of *King et al.* [1987] illustrates why the existing geodetic data cannot distinguish between rapid slip beneath a deep transition depth and slower slip beneath a shallower transition depth). Because virtually all Parkfield seismicity, both background and aftershocks, occurs at depths shallower than 14 km (Figure 3), the shallower transition depth is easier to accept. However, *Thatcher* [1979] and *Sieh and Jahns* [1984] presented geologic evidence that long-term deep slip rates of 33 mm/yr are more appropriate, in which case SH need the deeper transition depth to fit the data.

The estimated time to reaccumulate a moment deficit equivalent to the moment of the 1966 Parkfield earthquake varies depending on which combination of transition depth and deep slip rate is preferred. Figure 5a shows the range of moment estimates for the 1966 event and moment deficit rates since 1966. Figure 5b illustrates dates for the next Parkfield earthquake estimated by dividing the moment estimates by the moment deficit rates. All of these studies found that there is now stored moment equivalent to the moment of the 1966 earthquake. SH found that the time required to reaccumulate moment could be as long as 29 years but only if a deep slip rate of 22 mm/yr or less is assumed. Models based on the preferred slip rate of 33 mm/yr estimate that there was sufficient stored moment for another 1966 type event by 1986.

*Thatcher and Segall* [1990] arrived at even shorter estimates of the time required to reaccumulate strain. Assuming the deep slip rate to be known as 33–35 mm/yr, they determined that the time required for each geodetic line to recover its 1966 coseismic offset was 12 ± 2 years, averaged over all lines in the network. Although this technique requires the deep slip rate to be known and also assumes that the present "locked patch" coincides with the earthquake rupture zone, it is otherwise independent of the slip distribution. Thatcher and Segall also explored the effect of assuming that the fault plane is completely locked between 2 km and a transition depth and found that for such a model a transition depth of 14 km and a deep slip rate of 33 mm/yr fit the data. This model yields a coseismic slip of 400 mm. For a completely locked patch, the time to reaccumulate moment deficit equal to the 1966 event is simply the coseismic slip divided by the deep slip rate, or 12 years.

Thus most strain budget arguments suggest the moment deficit accumulated at Parkfield since 1966 is already equivalent to another magnitude 6 earthquake. However, this moment deficit is only a necessary, not a sufficient, condition for another 1966-like event. Additional moment being accumulated could either be released in a slightly larger rupture than in 1966 or could be added to the slip budget for an event that ruptures further south, as will be discussed below.

Could interaction with other faults have a significant effect on the Parkfield strain budget? *Simpson et al.* [1988] calculated the stress changes on the San Andreas fault northwest of Parkfield produced by the magnitude 6.7 Coalinga earthquake of 1983, which retarded surface creep near Middle Mountain for about a year [*Poley et al.*, 1987]. They showed that the Coalinga earthquake imposed left-lateral shear stresses and extensional normal stresses on the San Andreas fault plane at the anticipated hypocenter of the next Parkfield earthquake. If the coefficient of friction is high, then the reduction in normal stress would have been expected to advance the date of the next Parkfield earthquake, but if it is low, then left-lateral shear stress would explain a delay of the next Parkfield earthquake by as much as a year or two. About the same amount of delay was calculated by *Tullis et al.* [1990], whose model incorporated a state- and rate-dependent frictional sliding law.

A slowing over time of the slip rate below seismogenic depths might also explain a lengthening recurrence interval for Parkfield. *Ben-Zion et al.* [1991] have shown that such slowing would be expected as an aftereffect of the 1857 Fort Tejon earthquake southeast of Parkfield. However, by the present time the expected deceleration of deep slip would be lengthening successive interevent intervals by only 1–2 years.

## POTENTIAL FOR RUPTURE FARTHER SOUTH

Southeast of the Parkfield segment lies the rupture zone of the great 1857 Fort Tejon earthquake. This magnitude 8 earthquake ruptured the Cholame, Carrizo, and Mojave segments of the San Andreas fault (Figure 6) and, possibly, the Parkfield segment as well. Reports from contemporary residents indicate there were at least two foreshocks in the hours before the mainshock, probably magnitude 5–6 events in the Parkfield-Cholame area [*Sieh*, 1978*b*]. Consequently, there is concern that the next Parkfield earthquake could herald or be part of a larger event rupturing further south along the San Andreas fault.

It is generally agreed that slip on the Carrizo segment was at least 6.8 m in 1857, and since steady deep

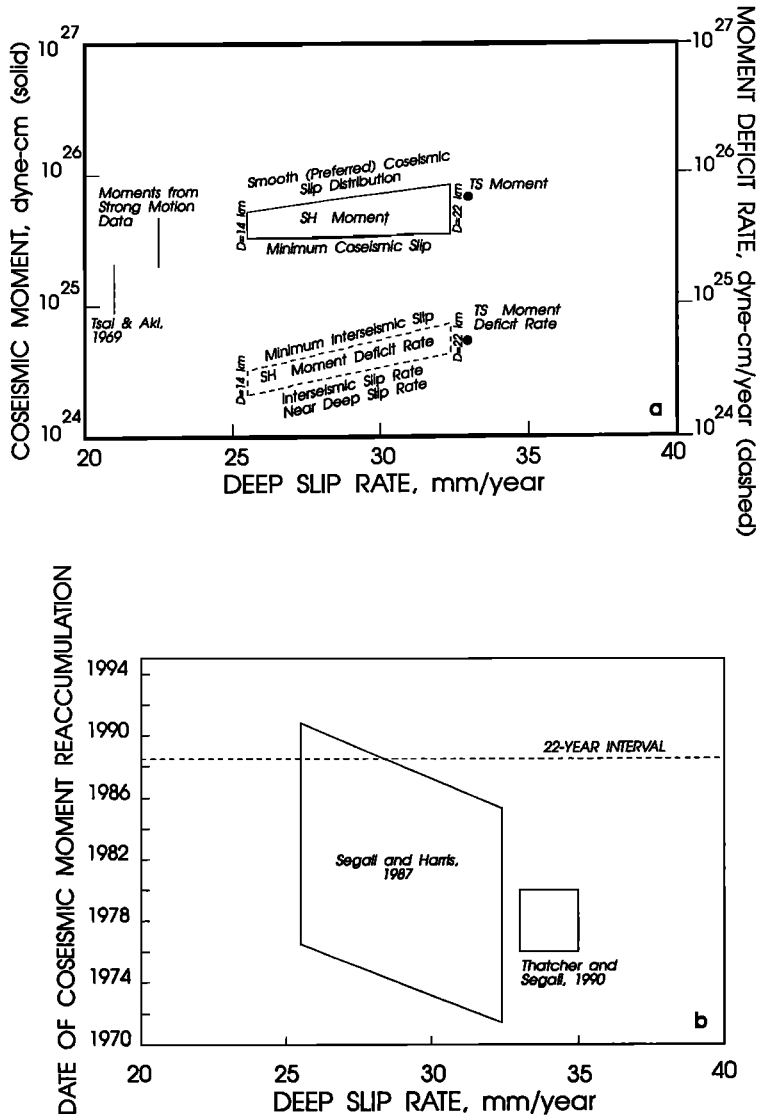


**Figure 5.** (a) Coseismic moments for the 1966 Parkfield earthquake and interseismic moment deficit rates, as estimated from geodetic and other types of data. Estimates based on geodetic data depend on the assumed deep slip rate. SH indicates estimates by *Segall and Harris* [1987]; TS indicates estimates by *Thatcher and Segall* [1990]. The moments determined by *Tsai and Aki* [1969] and those from strong motion data do not depend on the assumed slip rate. (b) Date when moment deficit reaches moment of 1966 Parkfield earthquake for models based on inversion of geodetic data.

slip at 30–35 mm/yr would have accumulated a slip deficit of only 4.0–4.7 m since 1857, a repeat of the 1857 event is unlikely at present. Although *Sieh et al.* [1989] estimated an average recurrence interval of 132 years for 10 earthquakes that ruptured the Mojave segment of the San Andreas fault, clusters of these events at intervals of less than a century were separated by longer repose intervals of 200–300 years. If the fault is now in a period of repose between clusters, then a full repeat of the Fort Tejon earthquake is unlikely this century. A Parkfield rupture probably could not trigger a Fort Tejon–size earthquake until the slip deficit needed for the larger event had reaccumulated.

However, the 55-km-long Cholame segment apparently experienced significantly less slip (probably less than 4 m) in 1857 than did the Carrizo segment. *Harris and Archuleta* [1987, 1988] inverted geodetic data to demonstrate that 30 km of the Cholame segment are locked to a depth of 15 km. If that segment has been locked since 1857, then it has now accumulated a slip deficit of 4 m or more, probably surpassing the 1857 slip on this segment as determined by *Sieh* [1978*a*].

On the Parkfield segment, Harris and Archuleta point out that SH's preferred model with a 14-km transition depth had coseismic slip of 0.34 m, with 8 mm of slip per year in the interseismic period if the deep slip rate is assumed to be 25 mm/yr (both these figures are averaged over the rupture zone). Assuming all known Parkfield earthquakes involved this amount of slip and that the interseismic slip rate has been constant since 1857, there would now be an accumulated slip deficit of at least 1.2 m on the Parkfield segment if the deep slip rate is 30 mm/yr. Harris and Archuleta believe the next Parkfield earthquake could release not only the same amount of slip as in 1966, but also the full 1.2-m deficit since 1857. If such an event also triggered 4 m of slip on the Cholame segment, the magnitude of the resulting earthquake would be 7.2, as estimated from its moment. In plausible histories of slip on the southern San Andreas fault, the Cholame segment has never ruptured without accompanying

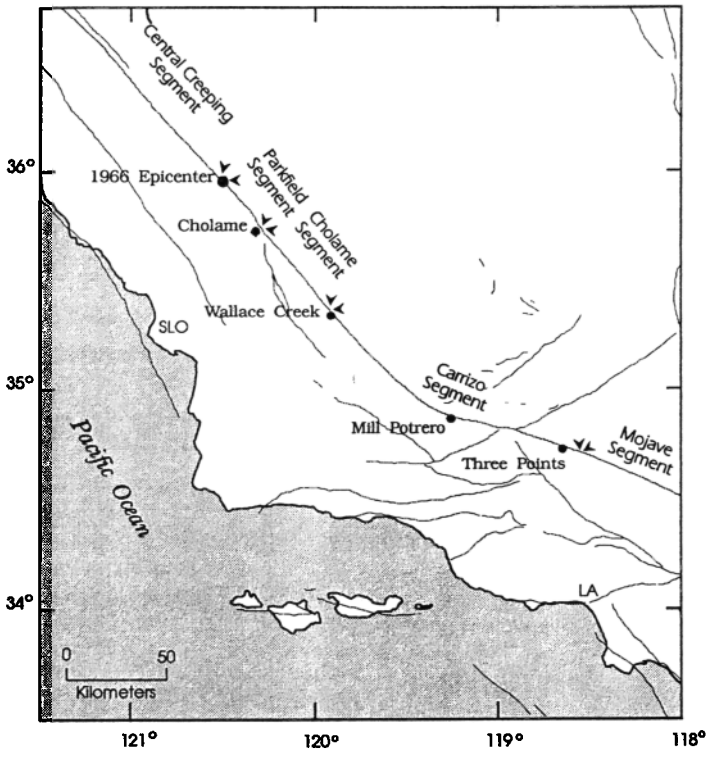


**Figure 6.** San Andreas fault segments [after *Sieh et al.*, 1989].

movement on the Carrizo segment [*Sieh et al.*, 1989], and an event in 1830 that damaged the mission in San Luis Obispo is the only historical event that might have represented a rupture of the Cholame segment by itself (J. Sims, personal communication, 1991). However, rupture of the Parkfield and Cholame segments together would be consistent with the present strain budget.

*Huang and Turcotte* [1990] studied two interacting rider-spring models with velocity-weakening friction laws as an analogue to the interaction of the Parkfield segment and the rupture zone of Fort Tejon earthquake, which they treat as a single segment on which an event with about 8 m of slip typically recurs every 132 years. This system behaves chaotically but in a fashion similar to scenarios described above. The block generating small events (analogous to the Parkfield segment) experiences several events, none of which completely relieves accumulated strain energy, before either slipping together with the other block in a larger event or triggering slightly delayed slip of the larger block. The repeat times between small events often became irregular before events involving the large block. Huang and Turcotte found model parameters such that the ratio of coseismic slip in the major event to that of the small event and the ratio of repeat times for the two types of events agreed with the parameters cited above for the 1857 earthquake and with a 22-year average Parkfield recurrence interval for an event with 0.56 m of slip. According to this model, the loss of regularity in interevent intervals suggests that the next Parkfield earthquake could involve rupture to the southeast and therefore be a much larger event.

The next Parkfield earthquake may have more capability to trigger a rupture further south if it relieves the total slip deficit accumulated since 1857, especially if the 1-km jog in the fault trace south of Gold Hill is indeed ineffective as a barrier to dynamic rupture. It seems unlikely that the next Parkfield earthquake could trigger a Fort Tejon–like event, because the accumulated slip deficit on the Carrizo and Mojave segments is not yet sufficient. Rupture of the Cholame segment, however, seems plausible, since its present slip deficit equals some estimates of its slip in 1857.

## NUMERICAL SIMULATIONS OF THE PARKFIELD EARTHQUAKE CYCLE

In addition to anecdotes of precursory fault slip before the 1966 Parkfield earthquake, numerical simulations of the earthquake process suggest that the next Parkfield earthquake may be preceded by measurable fault slip.

Computer models developed for Parkfield share certain basic features. They treat the fault as a vertical plane in an elastic half-space, with the part of the fault plane representing the Parkfield rupture zone (Figure 7) divided into a grid. Constant slip rate boundary conditions are imposed at the northwestern end of the Parkfield rupture zone and below a transition depth, while southeast of the Parkfield rupture zone the fault is assumed to move only in great earthquakes.

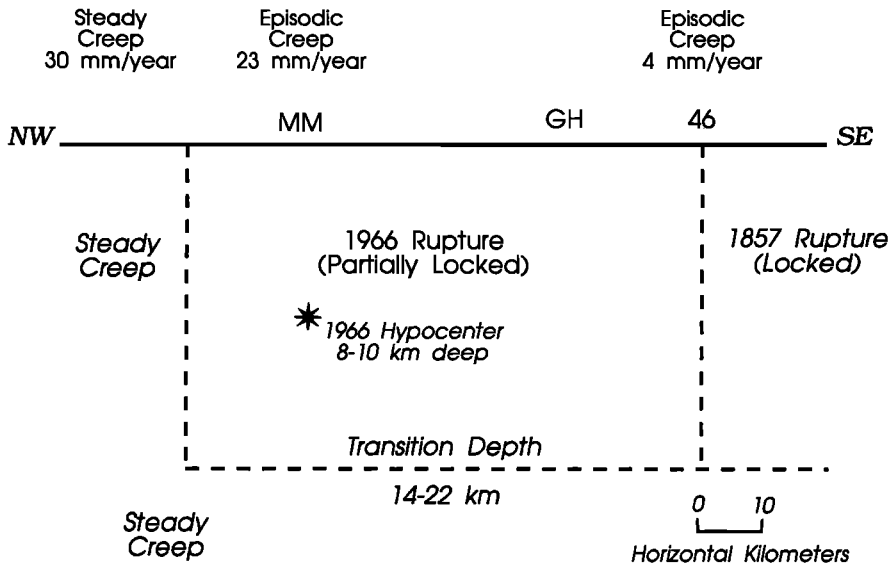


**Figure 7.** Schematic cross section looking northeast into the plane of the San Andreas fault, showing the general boundary conditions imposed on numerical simulations of the Parkfield earthquake cycle. MM is Middle Mountain; GH is Gold Hill; 46 is Highway 46. The depth scale is approximate. Historic slip rates are from *Lienkaemper and Prescott* [1989].

As time steps forward in the model, slip on any one grid cell changes the stress state on all of the other cells by an amount usually calculated using rectangular dislocation solutions for an elastic half-space [e.g., *Okada*, 1992]. In response to the changed stress, other cells may also slip. The stress threshold for slip and the amount of relative slip across each cell are governed by a frictional sliding law, which is the chief feature that differs from model to model. The frictional characteristics of the fault plane are adjusted to match the average 22-year recurrence interval for Parkfield.

*Stuart et al.* [1985] presented the first such model. The frictional behavior of the fault was modeled so that it could slip freely at a specified yield stress everywhere except in a relatively strong patch representing the "Parkfield asperity." Within this asperity the shear stress resisting fault slip was assumed to increase with increasing slip up to a peak stress and then to fall. In such a material, frictional instability occurs when the stress transferred from slipping cells to some part of the fault plane cannot be supported because the shear strength there has passed its peak and is falling too rapidly. Such an instability constitutes a simulated earthquake. The location and size of the patch representing the Parkfield asperity, its peak shear stress, a "characteristic" amount of slip required for stress to fall by a factor of $e^{-1}$ after passing the peak stress, and the boundaries of the 1857 "locked" patch were estimated from creep meter records and one trilateration line crossing the fault just northwest of Parkfield. The best fit to these data was obtained with a peak shear stress of 26 bars, a characteristic slip of 87 mm, and a patch 6 km in diameter centered 5 km beneath the town of Parkfield. The model was driven by a regional shear stress increasing constantly at 0.11 bar/year. This simulation predicted that during the last 1–3 years before the next Parkfield earthquake, accelerating slip prior to instability would produce detectable acceleration of fault creep at the surface. Stuart et al. explored the range of models that fit the creep and trilateration data and found that the models were consistent with the next Parkfield earthquake occurring in 1987 ± 8 years.

*Tullis and Stuart* [1992] have adapted Stuart et al.'s model to incorporate a state- and rate-dependent frictional constitutive law [*Dieterich*, 1979*a*, *b*; *Ruina*, 1983; *Blanpied et al.*, 1987]. The imposed slip rate at depth and in the creeping zone is 35 mm/yr. This model predicts that accelerating slip in the hypocentral region should precede the next Parkfield earthquake, and the volumetric strain at the surface caused by the slip might be as large as 5–40 nanostrain in the several days preceding the earthquake. This amount of strain could be detected by the Parkfield borehole strain array. Preseismic slip would not be expected to reach the surface, however, so that precursory signals on creep meters would not be expected.

*Ben-Zion and Rice* [1993] developed a model assuming that slip is steady at 35 mm/yr below 17.5 km depth and in the creeping section northwest of Parkfield. This model extends further northwest along the San Andreas fault than the other models in that it includes the rupture zone of the 1906 San Francisco earthquake. The rupture zones of the 1906 and 1857 earthquakes are represented by patches that slip every 150 years. In this model, the Parkfield "asperity" extends the length of the 1966 rupture zone between depths of 5 and 10 km. Every grid cell (cells are about 550 m on each side) that is not constantly slipping or in the 1906 or 1857 rupture zones has the same static shear strength, but the stress remaining after frictional failure is lower within the asperity than outside of the asperity. Thus failures within the asperity are characterized by higher stress drops than failures elsewhere on the fault plane. This feature is suggested by an observation by *O'Neill* [1984] that among Parkfield

microseismicity some events near the 1966 hypocenter had unusually high stress drops. Among a number of assumed stress drop distributions, the one best matching the observed 22-year average recurrence interval had a static strength of 60 bars, with stress drops of 54 bars and 12 bars in the asperity and nonasperity regions, respectively. If this stress drop distribution is used, this model simulates seismicity with realistic Gutenberg-Richter statistics; superimposing a random variation of stress drop from cell to cell smooths the frequency-magnitude relation. Although the average recurrence interval for magnitude 6 earthquakes was 22 years, the individual events were irregularly spaced in time and were preceded by nonrepeating patterns of foreshocks.

## EVIDENCE FOR STEADY STRAIN ACCUMULATION AT PARKFIELD

Geodetic data recorded at Parkfield to date are largely consistent with steady relative displacement across the San Andreas fault below the Parkfield rupture zone and permit the interpretation of a "locked patch" on some part of the fault that ruptured in the 1966 earthquake.

*King et al.* [1987] used geodetic data on many length scales from 1959 to 1984 to constrain the 1966 coseismic slip and the deep slip rate beneath the Parkfield segment (their preferred value is 33.4 ± 5 mm/yr below a depth of 16 km); they found all surveyed line lengths to be satisfactorily described as linear functions of time, indicating a steady rate of strain accumulation. Trilateration measurements since 1984 show no departure from this steady rate (M. Lisowski and N. King, oral communication, 1992).

*Langbein et al.* [1990] show that virtually all of the two-color geodimeter line length measurements from 1984 to 1988 can be explained by steady slip on the main strand of the San Andreas fault plus, on some lines, a variation with a period of 1 year that may be associated with rainfall. *Langbein et al.* [1990] judged excursions from this model to be only marginally significant relative to the measurement noise, although *Wyss et al.* [1990*b*] cited decreased deformation rates on two lines to support the hypothesis of seismic quiescence (see below). Measurements since 1988 do not change this picture.

Of eight borehole volumetric strain meters at Parkfield [*Sacks et al.*, 1971], six are still operational. One of these extremely sensitive instruments has clearly detected extensional steps of 5–10 nanostrain at the times of creep events on Middle Mountain. Coseismic strain steps have been recorded for the 1989 Loma Prieta and 1992 Landers earthquakes, as well as for two events of magnitude 4.0 and 4.7 in the Parkfield area, and are generally consistent with elastic dislocation models of these earthquakes. However, while other excursions have been observed, none have reached the lowest alert/status criterion of 0.1 microstrain change in one week recorded on at least two borehole strain meters. Because the data record an exponentially decreasing long-term compression due to curing of the grout that holds them in place, they cannot be used to measure the background rate of strain accumulation. However, excursions about the background rate can be detected and appear to be small.

Fault creep measurements [*Schulz*, 1989; K. S. Breckenridge, personal communication, 1992] show that since 1990, creep has slowed near Gold Hill and has possibly accelerated slightly at Middle Mountain while the seismicity rate was higher (see below). Although numerous creep events have met alert thresholds, no network-wide acceleration of creep rates has been observed.

Data from the USGS Parkfield Dense Seismograph Array [*Fletcher et al.*, 1992], which comprises 14 three-component stations in a 1-km$^2$ area, has been used to monitor coda $Q$ from small earthquakes in Parkfield since 1989. So far, no significant variation in coda $Q$ has been detected [*Hellweg et al.*, 1992].

## GEOPHYSICAL ANOMALIES AT PARKFIELD, 1984 TO OCTOBER 1992

Most instrumentation at Parkfield was installed to detect signals that might indicate when the next earthquake was due. Few networks have been totally without activity; Figure 8 shows the time history of Parkfield alert levels, and Table 2 lists the events resulting in B alert/status or higher that have occurred to date. Creep events, water level changes associated with them, and small earthquakes beneath Middle Mountain caused most of the level D and C episodes. In addition to the events listed in Table 2, several of the networks for which no alert/status levels are defined have recorded signals that can clearly be distinguished from noise. Most of these signals are small and do not unambiguously demonstrate aseismic slip near the expected hypocenter. Fluctuations in the seismicity rate as well as large, abrupt water level changes associated with fault creep resemble phenomena interpreted as earthquake precursors in other areas. The most publicized of these phenomena was an apparent decrease in seismicity rate ("quiescence") which has now been demonstrated to have been due to artificial changes in the magnitude scale. Below we describe some of these anomalous signals, most of which remain unexplained.

### "Quiescence"

Two groups perceived the onset of seismic quiescence at Parkfield in 1986 for events magnitude 2 or greater [*Aviles and Valdes*, 1989; *Bodin et al.*, 1989; *Wyss et al.*, 1990*a*]. *Wyss et al.* [1990*a*] argued that

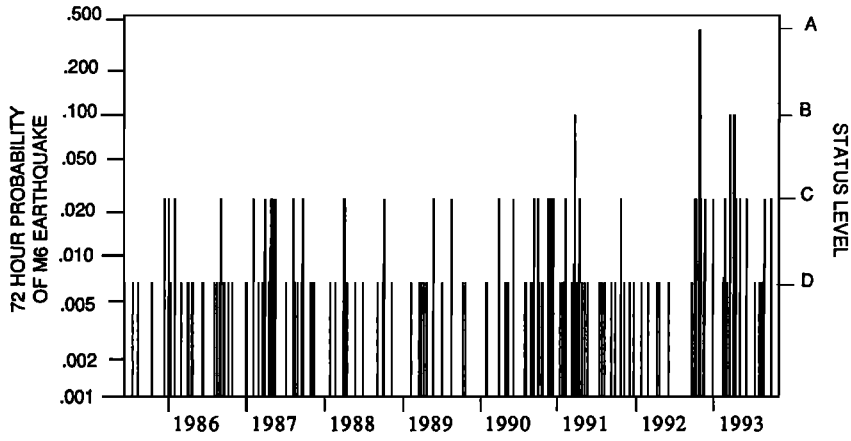


**Figure 8.** Graph showing the time history of alert/status levels for the Parkfield earthquake prediction experiment. Each period for which the status is D or higher is shown as a vertical bar. See Table 2 for fuller descriptions of level B and A alerts.

a 1.5-year quiescence had preceded one of the largest earthquakes in Parkfield since 1980 (August 29, 1986, magnitude 3.7) and that 4.5 years of quiescence were likely to precede the next Parkfield mainshock. This reasoning predicted that the Parkfield earthquake should have happened around 1990 and no later than March 1992, a prediction that was not fulfilled.

Wyss and his coworkers searched for other signals that might be related to the quiescence; *Wyss et al.* [1990*b*] reported a decrease in the rate of fault slip as measured by the two-color laser geodimeter beginning in September 1986. On the other hand, *Langbein et al.* [1990] had previously examined the same data set and did not report such a rate change; *Langbein* [1991] found the rate change reported by *Wyss et al.* [1990*b*] to be significant only at the 80% confidence level and that a more significant rate change had taken place in 1987.

*Wyss* [1990] also detected a decrease in average magnitude (reflected in a *b* value increase from 1.1 to 1.4) between late 1986 and late 1988, and *Wyss* [1991] showed that the mean depth of earthquakes in the northern and southern parts of the Parkfield rupture zone has increased by about 1 km starting around 1986.

*Stuart* [1991] suggested that quiescence as well as a deformation rate decrease could stem from the activation of aseismic slip on a subhorizontal "buffer fault" extending east and possibly west from the San Andreas fault at a depth of about 10 km. Stuart hypothesized that the buffer faults began to slide aseismically late in the earthquake cycle and was able to match *Wyss et al.*'s [1990*b*] geodetic rate decrease with a model including slip on them.

Magnitudes in the USGS Calnet catalog, which have been computed by several different methods over the years, were the basic data used to demonstrate the existence of quiescence at Parkfield. Before publications on Parkfield quiescence appeared, USGS staff seismologists warned that the magnitude scale changes probably affected the apparent seismicity rate, but they did not demonstrate until 1992 that the quiescence was an artifact of these changes. Thus Parkfield has not tested the hypothesis that quiescence is an intermediate term earthquake precursor, and the existence and significance of other changes associated with the apparent quiescence are being reevaluated.

### Seismicity Increase

Even taking into account magnitude scale changes, Parkfield seismicity began to increase in August 1990 (Figure 9). On August 2, a magnitude 3.1 earthquake took place south of the town of Cholame. This earth-

**TABLE 2. Parkfield Events Leading to Level B or Higher Status Since the Beginning of the Experiment**

| *Date* | *Location* | *Description* | *Size* | *Level* | *Comments* |
|---|---|---|---|---|---|
| March 19, 1991 | XPK1 and XVA1 | creep | 5 mm in 16 hours (right-lateral) | B | raining |
| Oct. 20, 1992 | South end, Middle Mountain | earthquake | magnitude 4.7 | A | coseismic steps |
| Oct. 26, 1992 | South end, Middle Mountain | earthquake | magnitude 3.4 and 3.9 | B | 2 km NW of Oct. 20 event |
| March 13, 1993 | Middle Mountain | earthquake | magnitude 3.5 | B | Same hypocenter as Oct. 26 event |
| April 3, 1993 | Middle Mountain | earthquake | magnitude 4.4 | B | 2 km shallower than Oct. 20 event |

In addition to the A alert and four B alerts there have been 42 C status and 109 D status episodes.

quake, several kilometers south of the southern end of the 1966 rupture zone, was the largest earthquake in that area since 1975. On August 28, a magnitude 2.9 earthquake occurred in nearly the same location. Intriguingly, both of these earthquakes had normal fault focal mechanisms, with nodal planes striking approximately north-south. Calnet recorded 33 events with magnitude 1.1 or greater in August, about twice the usual number of events per month during the previous several years.

On September 9 and 10 there were magnitude 3.3 earthquakes in the northern part of the Parkfield rupture zone; both were in locations that had been active clusters in the past. The second event had a thrust focal mechanism, and was the deepest earthquake since 1975 in the portion of the fault immediately north of Middle Mountain. There were 32 events in the Parkfield area during September.

On November 14 there was a magnitude 3.2 earthquake within 1 km of the hypocenter of the 1966 Parkfield earthquake. Events of this size in this location were not infrequent before 1982; a magnitude 3.2 earthquake took place on June 27, 1982, in almost exactly the same place. However, since then there had been no other earthquake that large and that close to the hypocenter of the 1966 event. Calnet recorded 26 events in the Parkfield area during November, the fourth consecutive month with an above average number of events. By early December it could be shown that the rate increase was statistically significant at the 95% confidence level. However, by mid-1992 the number of events per month had returned to between 16 and 22, typical of the period before August 1990.

### Creep Events and Water Level Changes

Many water level changes have been recorded in a well on Middle Mountain, 400 m from the creeping fault trace, since monitoring of the well began in 1987. The water level changes range in size from a few centimeters to 20 cm (corresponding to aquifer strain changes up to 0.27 microstrain) and coincide with fault creep events recorded at two creep meters on Middle Mountain, northwest and southeast of the well. Some of these events are also accompanied by strain steps of 3–10 nanostrain recorded on borehole strain meters, suggesting that the events represent slip to a depth of no more than 1 km. Several such changes have been observed every year, and although they resemble phenomena believed to have been earthquake precursors in other places, none of these water level drops has been followed by the magnitude 6 Parkfield earthquake [*Roeloffs*, 1989].

### Resistivity

*Park* [1991] reviews previous examples of resistivity changes believed to be of tectonic origin and describes the Parkfield telluric array, which consists of eight passive dipoles 5–18 km long, each of which connects two electrodes where voltage is measured (Figure 10). Two approximately orthogonal dipoles are chosen as references, and six pairs of "telluric coefficients" are estimated from the data daily. Each pair of telluric coefficients expresses the voltage across one of the nonreference dipoles in terms of that across each of the two reference dipoles. *Park and Fitterman* [1990] showed that a 1% change in resistivity between depths of 1 and 5 km beneath the array should result in a 1% change in some of these coefficients, which is approximately the smallest change that can be detected. Since the array began operation in 1988, several fluctuations above the noise level have been detected. The largest fluctuation, in April 1989, was observed on two dipoles and could be explained by 10.5–17.5% changes of resistivity beneath the array. *Park* [1994] demonstrates the statistical significance of this anomaly. Interestingly, this fluctuation coincided with shear strain anomalies of 180 and 100 nanostrain, respectively, at the Donalee and Eades tensor strain meters (Figure 10). However, the resistivity change needed to account for the observed telluric coefficient fluctuations is 2 orders of magnitude larger than would be expected from the tensor strain record using laboratory measurements of the sensitivity of resistivity to strain. It may be significant that a magnitude 3.7 earthquake occurred near the southern end of the Parkfield rupture zone about 1 month after these resistivity and tensor strain anomalies. Moreover, a travel time anomaly was noticed on a Vibroseis waveform path passing through one of the affected dipoles.

### Vibroseis Wave Propagation Changes

Several times per year since mid-1987 the seismic signal from a shear wave vibrator has been recorded at each of nine three-component borehole seismometers and in a vertical three-component borehole array [*Michelini and McEvilly*, 1991; *Karageorgi et al.*, 1992]. Records from eight vibrator positions are examined for changes in waveform with time that may correspond to physical changes beneath the epicenter of the 1966 Parkfield earthquake, a volume many of the ray paths traverse. Shear wave splitting indicates shear wave anisotropy in the fault zone, confirming an earlier study by *Daley and McEvilly* [1990] based on data collected from the vertical array. On several paths within 5 km to the southwest of the 1966 epicenter, a progressive travel time decrease of 3 to 7 ms/yr has been observed for a phase that arrives 7–11 s into the wave train. On a path extending 9 km southeast along the fault trace from the 1966 epicenter, temporary variations in $P$ wave travel time of up to 40 ms took place in May–June 1989 and in the first half of 1990. The May–June 1989 episode coincides spatially with the resistivity change reported by *Park* [1991] and follows that anomaly by only 1 month (Figure 10).

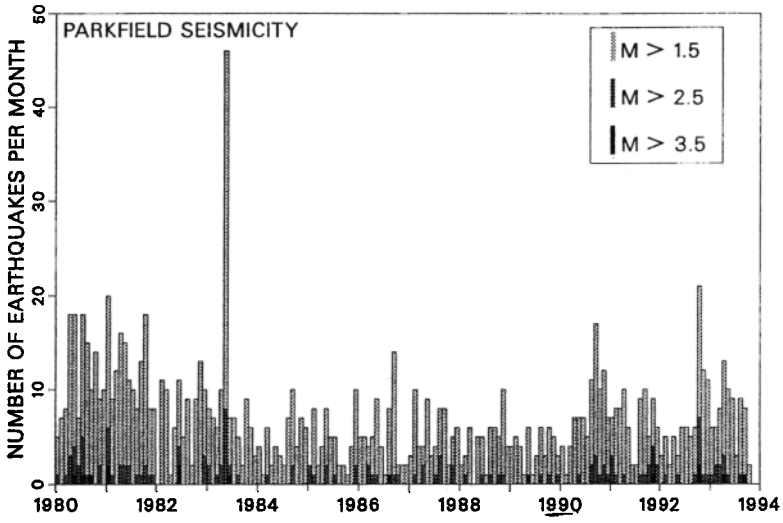


**Figure 9.** Bar graph showing the number of earthquakes per month recorded by Calnet near Parkfield.

### Magnetometers

Seven proton precession magnetometers, forming a differentially connected array, have been operating at Parkfield since 1985. *Mueller et al.* [1994] summarize results through January 1992 and note that a gradual increase of 0.5 nT/yr began in 1989 at one magnetometer near the southeastern end of the Parkfield rupture zone and continues to the present.

### Seismicity Migration

*Malin and Alvarez* [1992] examined earthquakes of magnitude 0 and greater recorded by the borehole seismometer network and showed that an abrupt increase in cumulative seismic moment took place in May 1990 for earthquakes north of Middle Mountain. In a 28-km-long box at the northern end of the Parkfield rupture zone, a similar increase was observed later, in September 1990, and south of the 1966 rupture zone the increase took place later yet, in January 1991. Malin and Alvarez interpreted this progression as evidence of a southeastwardly moving stress front traveling 30–50 km/yr.

## FIRST LEVEL "A" ALERT IN OCTOBER 1992

A magnitude 4.7 earthquake on October 20, 1992 (Figure 11), brought the Parkfield experiment to its first level A alert, which expired 72 hours later without the occurrence of a larger earthquake. This was the first level A alert since the Parkfield experiment began in 1985 (Figure 8), and it is described in detail by the *Parkfield Working Group* [1993]. Parkfield alert levels are designed so that A level alerts should be expected approximately once every 55 months, with about two of every three being "false alarms." Thus the nonoccurrence of a magnitude 6 earthquake during this alert period was not unexpected.

On October 26 a magnitude 3.9 event occurred slightly to the northwest of the October 20 event (Fig-

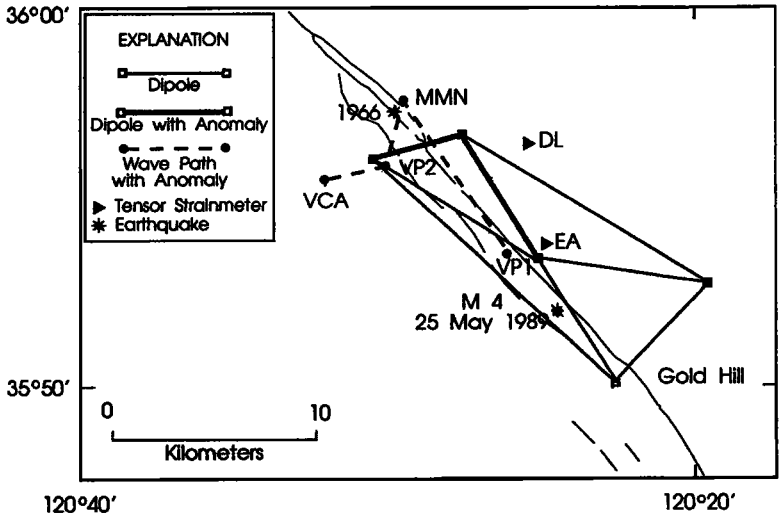


**Figure 10.** Map showing locations of telluric dipoles and borehole tensor strain meters (DL is Donalee; EA is Eades) that recorded anomalies in April 1989 [*Park*, 1991]. Vibroseis paths with travel time anomalies are also shown; the path from MMN to VP1 displayed an anomaly in May–June 1989; the paths from VP2 to VCA and MMN display a progressive travel time increase for a late-arriving phase [*Karageorgi et al.*, 1992]. Location of the magnitude 4 earthquake in May 1989 is also shown.

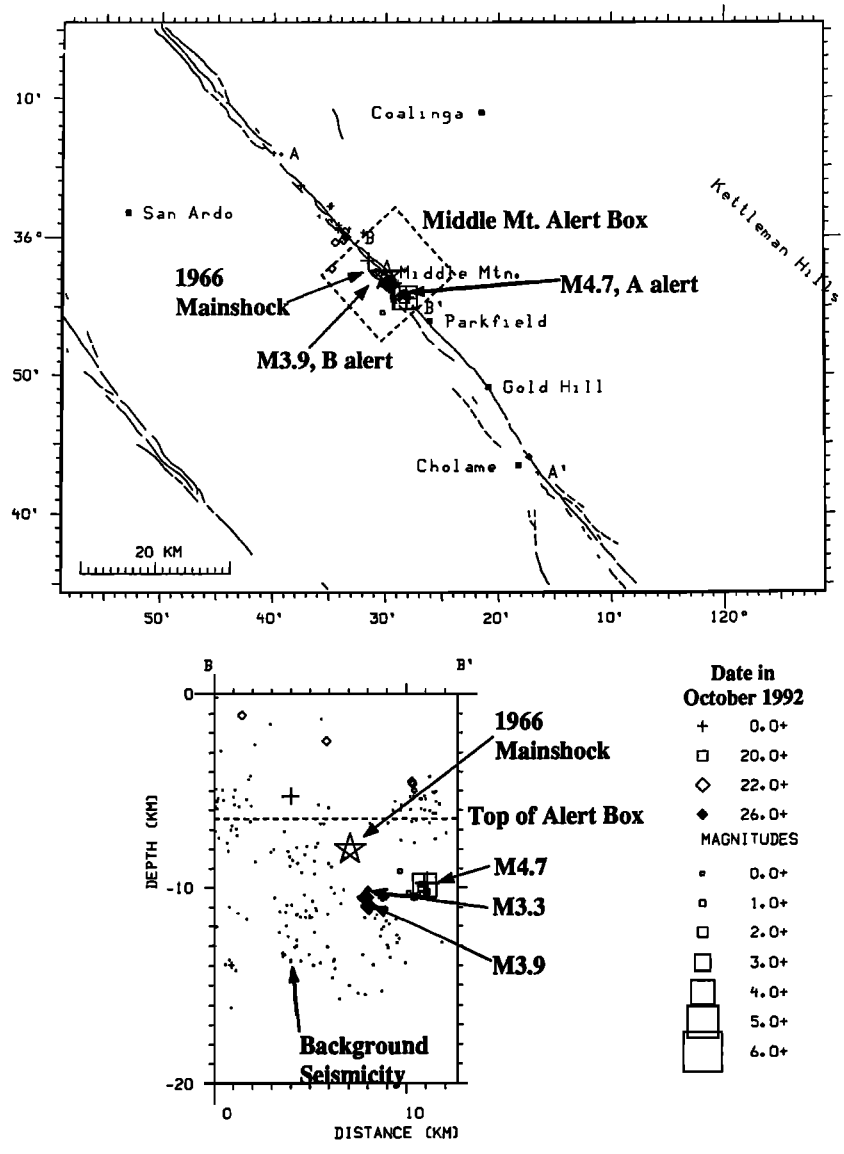


**Figure 11.** Map and cross-section views of earthquakes during the October 1992 level A Parkfield alert [from *Parkfield Working Group*, 1993].

ure 11), meeting a criterion for a level B alert that lasted until October 29. Further earthquakes of magnitudes between 1.5 and 2.0 followed, causing the experiment to remain at status C until October 31.

Compared with foreshocks of the 1934 and 1966 Parkfield earthquakes, the October 20 event occurred 5 km southeast of their common location and was smaller than those events. Among magnitude 4.5–5.0 Parkfield earthquakes that have been recorded by a Wood-Anderson seismograph in Berkeley, California (excluding aftershocks), the October 20 event most closely resembled a magnitude 4.5–4.6 earthquake on January 5, 1975, which was not followed by a larger Parkfield earthquake. Nevertheless, its aftershock distribution and azimuthal variation of apparent source duration show that the October 20 event was a northwestward propagating rupture, like past Parkfield foreshocks. The October 20 event was estimated to have increased shear stress at the hypocenter of the 1966 Parkfield earthquake by approximately 0.15 bars, equivalent to about 2 months of stress buildup at the background rate of 1 bar/yr estimated by *Segall and Harris* [1987]. Although similar stress changes were presumably imposed by the 1975 magnitude 4.6 earthquake, the changes due to the magnitude 4.7 event on October 20 are superimposed on a stress state that most plausible models show to now be critically stressed.

Other than seismometers, no instruments at Parkfield recorded any unusual signals in the 12 days prior to the magnitude 4.7 earthquake. However, speculation quickly emerged as to whether a sequence of accelerated fault creep episodes between October 1 and October 4, followed by magnitude 2.5 and 2.7 earthquakes on October 4 and October 7, may have foreshadowed the event that produced the A level alert. This fault creep took place directly above the hypocenter of the magnitude 4.7 earthquake, and the October 4–7 seismicity occurred very nearly at the same location as that event [*Michael et al.*, 1993]. A

13-cm water level drop and an extensional strain step of 10 nanostrain accompanied the early October creep sequence, but as was noted above, such signals have been observed many times before at Parkfield. The sequence of creep episodes itself is similar in amplitude and event duration to eight others that have taken place since the Parkfield creep meter network was completed in 1988, but only one of the other eight creep sequences was followed by earthquakes directly beneath the active creep meters [*Breckenridge*, 1993]. At this time, the only apparent distinctive feature of the early October creep sequence that might link it to the magnitude 4.7 earthquake is the near-simultaneous occurrence of earthquakes in the same location as the October 20 magnitude 4.7 event.

## SUMMARY

The nonoccurrence of the next magnitude 6 Parkfield earthquake before the end of 1992 suggests that the recurrence interval distribution proposed by *Bakun and Lindh* [1985] is unrealistically narrow. The slightly broader Nishenko-Buland distribution estimates the probability of the Parkfield earthquake before 1995 as 30%. Using a distribution derived from the observed interevent intervals at Parkfield yields at most a 15% chance of having the earthquake before 1995, and if the additional events discovered by *Toppozada et al.* [1990] were really Parkfield earthquakes, then the recurrence interval distribution is even broader and the probability of an event by 1995 is even lower.

The definition of the Parkfield fault segment has been scrutinized. Contemporary microseismicity at Parkfield does not define the 5° bend or 1-km right step hypothesized to mark the ends of the Parkfield rupture zone. The northern end remains defined by the transition from steady to episodic creep and the abrupt decrease in shallow seismicity. Geologic evidence suggests that structures near the right step at the southern end of the rupture zone are actively evolving and may not act to arrest the next Parkfield rupture in the same way as in 1966. On the other hand, features in the compressional velocity structure confirm that there are physical property changes at depth at the ends of the postulated Parkfield segment.

Models consistent with the geodetic data and the most plausible deep slip rate tell us that moment equivalent to that of the 1966 Parkfield event has already reaccumulated. Only new evidence that the deep slip rate is of the order of 22 mm/yr rather than 33–35 mm/yr would negate this conclusion. These models also suggest that Parkfield earthquakes do not relieve all of the slip deficit accumulated in the interseismic periods, and the models raise the possibility that the next event at Parkfield could be larger and more likely to trigger rupture further south than the 1966 event.

A much-reported period of seismic quiescence at Parkfield beginning in 1986 was later shown to be an artifact of a magnitude scale change. However, an increase in seismicity from August 1990 until early 1992 can be documented despite the scale change. Episodes of fault creep accompanied by water level changes and borehole strain meter signals occur routinely at Parkfield, and there has been an intriguing correspondence of borehole strain, travel time, and resistivity anomalies. On October 20, 1992, a magnitude 4.7 earthquake brought the Parkfield experiment to its first level A alert. However, none of these phenomena has yet proved to be a harbinger of the magnitude 6 earthquake.

**ACKNOWLEDGMENTS.** We thank the Parkfield Working Group, whose members are too numerous to list, for many enlightening discussions, often about unpublished work. We greatly appreciate the thoughtful comments of Jim O'Connor, Steve Park, J. C. Savage, and two reviewers.

Larry Ruff was the editor responsible for this paper. He thanks Alan Chave for a cross-disciplinary review and Steve Park and an anonymous referee for their technical reviews.

## REFERENCES

Aki, K., and P. G. Richards, *Quantitative Seismology: Theory and Methods*, 2 vols., W. H. Freeman, New York, 1980.

Allen, C. R., and S. W. Smith, Parkfield earthquake of June 27–29, 1966, Preearthquake and post-earthquake surficial displacement, *Bull. Seismol. Soc. Am.*, *56*, 955–967, 1966.

Archuleta, R. J., and S. M. Day, Dynamic rupture in a layered medium: The 1966 Parkfield earthquake, *Bull. Seismol. Soc. Am.*, *70*, 671–689, 1980.

Armstrong, B. H., and C. M. Valdes, Acoustic emission/microseismic activity at very low strain levels, in Acoustic Emission: Current Practice and Future Directions, edited by W. Sachse, J. Roget, and K. Yamaguchi, *ASTM Spec. Tech. Publ., STP 1077*, 358–364, 1991.

Aviles, C., and C. M. Valdes, Comparison of microearthquake source parameters in the preparation zone at Parkfield, California: 1977–1982 and 1984–1989 (abstract), *Eos Trans. AGU*, *70*, 1228, 1989.

Aviles, C. A., and A. J. Michael, Complications at the southern end of 1966 Parkfield rupture zone (abstract), *Eos Trans. AGU*, *71*, 1473, 1990.

Bakun, W. H., History of significant earthquakes in the Parkfield area, *Earthquakes Volcanoes*, *20*, 45–51, 1988*a*.

Bakun, W. H., Geophysical instrumentation near Parkfield, *Earthquakes Volcanoes*, *20*, 60–71, 1988*b*.

Bakun, W. H., The USGS plan for short-term prediction of the anticipated Parkfield earthquake, *Earthquakes Volcanoes*, *20*, 83–87, 1988*c*.

Bakun, W. H., and A. G. Lindh, The Parkfield, California, earthquake prediction experiment, *Science*, *229*, 619–624, 1985.

Bakun, W. H., and T. V. McEvilly, Earthquakes near Park-

field, California: Comparing the 1934 and 1966 sequences, *Science*, *205*, 1375–1377, 1979.

Bakun, W. H., and T. V. McEvilly, *P* wave spectra for $M_1$ 5 foreshocks, aftershocks, and isolated earthquakes near Parkfield, California, *Bull. Seismol. Soc. Am.*, *71*, 423–436, 1981.

Bakun, W. H., et al., Parkfield earthquake prediction scenarios and response plans, *U.S. Geol. Surv. Open File Rep.*, *86-365*, 37 pp., 1986.

Bakun, W. H., et al., Parkfield earthquake prediction scenarios and response plans, *U.S. Geol. Surv. Open File Rep.*, *87-192*, 45 pp., 1987.

Ben-Zion, Y., and J. R. Rice, Earthquake failure sequences along a cellular fault zone in a three-dimensional elastic solid containing asperity and nonasperity regions, *J. Geophys. Res.*, *98*, 14,109–14,131, 1993.

Ben-Zion, Y., J. R. Rice, and R. Dmowska, Interaction of the San Andreas fault creeping zone with adjacent great rupture zones, and earthquake recurrence at Parkfield (abstract), *Eos Trans. AGU*, *72*, 483, 1991.

Bernardi, A., A. C. Fraser-Smith, P. R. McGill, and O. G. Villard Jr., ULF magnetic field measurements near the epicenter of the $M_s$ 7.1 Loma Prieta earthquake, *Phys. Earth Planet. Inter.*, *68*, 45–63, 1991.

Blanpied, M. L., T. E. Tullis, and J. D. Weeks, Frictional behavior of granite at low and high sliding velocities, *Geophys. Res. Lett.*, *14*, 554–557, 1987.

Bodin, P., M. Wyss, and R. E. Habermann, The tempo of Parkfield seismicity: Allegro ma non troppo? (abstract), *Eos Trans. AGU*, *70*, 1230, 1989.

Borcherdt, R. D., J. B. Fletcher, E. G. Jensen, G. L. Maxwell, J. R. VanSchaack, R. E. Warrick, E. Cranswick, M. J. S. Johnston, and R. McClearn, A general earthquake-observation system (GEOS), *Bull. Seismol. Soc. Am.*, *75*, 1783–1825, 1985.

Borcherdt, R. D., M. J. S. Johnston, T. C. Noce, G. M. Glassmoyer, and D. Myren, A broadband wide dynamic range strong motion array near Parkfield, California, U.S.A., for measurement of acceleration and volumetric strain, paper presented at 9th World Conference on Earthquake Engineering, Int. Assoc. for Earthquake Eng., Tokyo/Kyoto, Japan, Aug. 2–9, 1988.

Breckenridge, K. S., Parkfield creep clusters and the level A alert: Precursor or pretender? (abstract), *Eos Trans. AGU*, *74*(16), Spring Meeting suppl., 379, 1993.

Brown, R. D., Jr., Map showing recently activated breaks along the San Andreas and related faults between the northern Gabilan Range and Cholame Valley, California, *U.S. Geol. Surv. Misc. Map Invest., Map, I-575*, 1970.

Daley, T. M., and T. V. McEvilly, Shear-wave anisotropy in the Parkfield Varian Well VSP, *Bull. Seismol. Soc. Am.*, *80*, 857–869, 1990.

Davis, P. M., D. D. Jackson, and Y. Y. Kagan, The longer it has been since the last earthquake, the longer the expected time till the next?, *Bull. Seismol. Soc. Am.*, *79*, 1439–1456, 1989.

Deng, Q., P. Jiang, L. M. Jones, and P. Molnar, A preliminary analysis of reported changes in ground water and anomalous animal behavior before the 4 February 1975 Haicheng earthquake, in *Earthquake Prediction: An International Review, Maurice Ewing Ser.*, vol. 4, edited by D. W. Simpson and P. G. Richards, pp. 543–565, AGU, Washington, D. C., 1981.

Dieterich, J. H., Modeling of rock friction, 1, Experimental results and constitutive equations, *J. Geophys. Res.*, *84*, 2161–2168, 1979*a*.

Dieterich, J. H., Modeling of rock friction, 2, Simulation of preseismic slip, *J. Geophys. Res.*, *84*, 2169–2175, 1979*b*.

Eaton, J. P., M. E. O'Neill, and J. N. Murdock, Aftershocks of the 1966 Parkfield-Cholame, California, earthquake: A detailed study, *Bull. Seismol. Soc. Am.*, *60*, 1151–1197, 1970.

Eberhart-Phillips, D., and A. J. Michael, Three-dimensional velocity structure, seismicity, and fault structure in the Parkfield region, central California, *J. Geophys. Res.*, *98*, 15,737–15,758, 1993.

Fletcher, J. B., L. M. Baker, P. Spudich, P. Goldstein, J. D. Sims, and M. Hellweg, The USGS Parkfield, California, dense seismography array: UPSAR, *Bull. Seismol. Soc. Am.*, *82*, 1041–1070, 1992.

Fraser-Smith, A. C., A. Bernardi, P. R. McGill, M. E. Ladd, R. A. Helliwell, and O. G. Villard Jr., Low-frequency magnetic field measurements near the epicenter of the $M_s$ 7.1 Loma Prieta earthquake, *Geophys. Res. Lett.*, *17*, 1465–1468, 1990.

Gladwin, M., R. L. Gwyther, R. Hart, M. F. Francis, and M. J. S. Johnston, Borehole tensor strain measurements in California, *J. Geophys. Res.*, *92*, 7981–7988, 1987.

Harris, R. A., and R. J. Archuleta, Slip deficit on the San Andreas fault: Potential for a magnitude 7 event at Parkfield (abstract), *Eos Trans. AGU*, *68*, 1350, 1987.

Harris, R. A., and R. J. Archuleta, Slip budget and potential for a *M*7 earthquake in central California, *Geophys. Res. Lett.*, *15*, 1215–1218, 1988.

Harris, R. A., and P. Segall, Detection of a locked zone at depth on the Parkfield, California, segment of the San Andreas fault, *J. Geophys. Res.*, *92*, 7945–7962, 1987.

Hellweg, M., P. Spudich, and J. B. Fletcher, Stability of coda *Q* at Parkfield, California (abstract), *Eos Trans. AGU*, *73*, 397, 1992.

Hill, D. P., M. J. S. Johnston, J. O. Langbein, S. R. McNutt, C. D. Miller, C. E. Mortensen, A. M. Pitt, and S. Rojstaczer, Response plans for volcanic hazards in the Long Valley Caldera and Mono Craters area, California, *U.S. Geol. Surv. Open File Rep.*, *91-270*, 1991.

Holzer, T. L., M. J. Bennett, T. L. Youd, and A. T. F. Chen, Parkfield, California, liquefaction prediction, *Bull. Seismol. Soc. Am.*, *78*, 385–389, 1988.

Huang, J., and D. L. Turcotte, Evidence for chaotic fault interactions in the seismicity of the San Andreas fault and Nankai trough, *Nature*, *348*, 234–236, 1990.

Hurst, K., et al., The first rapid static GPS survey of 107 monuments in the Parkfield CA area using TurboRogue receivers, *Eos Trans. AGU*, *73*(43), Fall Meeting suppl., 398, 1992.

Isenberg, J., E. Richardson, and T. D. O'Rourke, Experiment on performance of buried pipelines across San Andreas fault, *Tech. Rep. NCEER-89-0005*, Natl. Center for Earthquake Eng. Res., State Univ. of N. Y. at Buffalo, March 10, 1989.

Isenberg, J., E. Richardson, H. Kameda, and M. Sugito, Pipeline response to Loma Prieta Earthquake, *J. Struct. Eng. Am. Soc. Civ. Eng.*, *117*, 2135–2148, 1991.

Johnston, M. J. S., A. T. Linde, M. T. Gladwin, and R. D. Borcherdt, Fault failure with moderate earthquakes, *Tectonophysics*, *144*, 189–206, 1987.

Jones, L. M., Foreshocks (1966–1980) in the San Andreas system, California, *Bull. Seismol. Soc. Am.*, *74*, 1361–1380, 1984.

Jones, L. M., et al., Short-term earthquake hazard assessment for the San Andreas fault in southern California, *U.S. Geol. Surv. Open File Rep.*, *91-32*, 1991.

Karageorgi, E., R. Clymer, and T. V. McEvilly, Seismological studies at Parkfield, II, Search for temporal variations in wave propagation using Vibroseis, *Bull. Seismol. Soc. Am.*, *82*, 1388–1415, 1992.

King, N. E., P. Segall, and W. Prescott, Geodetic measure-

ments near Parkfield, California, 1959–1984, *J. Geophys. Res.*, *92*, 2747–2766, 1987.

Langbein, J., E. Quilty, and K. Breckenridge, Sensitivity of crustal deformation instruments to changes in secular rate, *Geophys. Res. Lett.*, *20*, 85–88, 1993.

Langbein, J. O., Earthquake explanations, *Nature*, *349*, 287, 1991.

Langbein, J. O., R. O. Burford, and L. E. Slater, Variations in fault slip and strain accumulation at Parkfield, California: Initial results using two-color geodimeter measurements, 1984–1988, *J. Geophys. Res.*, *95*, 2533–2552, 1990.

Lienkaemper, J. J., and W. H. Prescott, Historic surface slip along the San Andreas fault near Parkfield, California, *J. Geophys. Res.*, *94*, 17,647–17,670, 1989.

Lindh, A. G., and D. M. Boore, Control of rupture by fault geometry during the 1966 Parkfield earthquake, *Bull. Seismol. Soc. Am.*, *71*, 95–116, 1981.

Malin, P. E., and M. G. Alvarez, Stress diffusion along the San Andreas fault at Parkfield, California, *Science*, *256*, 1005–1007, 1992.

Malin, P. E., S. N. Blakeslee, M. G. Alvarez, and A. J. Martin, Microearthquake imaging of the Parkfield asperity, *Science*, *244*, 557–559, 1989.

McGill, P. R., A. C. Fraser-Smith, and R. A. Helliwell, Ultra-low frequency magnetic field measurements at Parkfield, California, during the level-A and level-B earthquake alerts of October 1992 (abstract), *Eos Trans. AGU*, *74*(16), Spring Meeting suppl., 379, 1993.

McJunkin, R. D., and A. F. Shakal, The Parkfield strong-motion array, *Calif. Geol.*, *36*, 27–34, 1983.

Michael, A. J., and D. Eberhart-Phillips, Relationships between fault behavior, subsurface geology, and three-dimensional velocity models, *Science*, *253*, 651–654, 1991*a*.

Michael, A. J., and D. Eberhart-Phillips, Fault geometry at the surface and at seismogenic depth near Parkfield, California (abstract), *Eos Trans. AGU*, *72*, 483, 1991*b*.

Michael, A. J., and J. Langbein, Earthquake prediction lessons from Parkfield, *Eos Trans. AGU*, *74*, 145, 153–155, 1993.

Michael, A. J., W. Ellsworth, G. Beroza, A. Cole, and K. Breckenridge, What caused the Parkfield A level alert?, *Eos Trans. AGU*, *74*(16), Spring Meeting suppl., 378, 1993.

Michelini, A., and T. V. McEvilly, Seismological studies at Parkfield, I, Simultaneous inversion for velocity structure and hypocenters using cubic B-splines parameterization, *Bull. Seismol. Soc. Am.*, *81*, 524–552, 1991.

Mortensen, C. E., E. Y. Iwatsubo, M. J. S. Johnston, G. D. Myren, V. K. Keller, and T. L. Murray, U.S.G.S. tiltmeter networks, operation and maintenance, *U.S. Geol. Survey Open File Rep.*, *77-655*, 1978.

Mueller, R. J., M. J. S. Johnston, J. O. Langbein, and K. S. Breckenridge, Local differential magnetic fields at Parkfield, California: July, 1985 to January, 1992, in Proceedings of the U.S.–People's Republic of China Workshop on Focused Earthquake Prediction Experiments, *U.S. Geol. Surv. Open File Rep.*, in press, 1994.

Myren, D., and M. J. S. Johnston, Borehole dilatometer installation, operation and maintenance at sites along the San Andreas fault, California, *U.S. Geol. Surv. Open File Rep.*, *89-349*, 1989.

Nishenko, S. P., and R. Buland, A generic recurrence interval distribution for earthquake forecasting, *Bull. Seismol. Soc. Am.*, *77*, 1382–1399, 1987.

Nishioka, G. K., and A. J. Michael, A detailed seismicity study of the Middle Mountain zone at Parkfield, California, *Bull. Seismol. Soc. Am.*, *80*, 577–588, 1990.

Noguchi, M., and H. Wakita, A method for continuous measurement of radon in groundwater for earthquake prediction, *J. Geophys. Res.*, *82*, 1353–1357, 1977.

Okada, Y., Internal deformation due to shear and tensile faults in a half-space, *Bull. Seismol. Soc. Am.*, *82*, 1018–1040, 1992.

O'Neill, M. E., Source dimensions and stress drops of small earthquakes near Parkfield, California, *Bull. Seismol. Soc. Am.*, *74*, 27–40, 1984.

Park, S. K., Monitoring resistivity changes prior to earthquakes in Parkfield, California, with telluric arrays, *J. Geophys. Res.*, *96*, 14,211–14,237, 1991.

Park, S. K., Quantification of errors for the Parkfield telluric array, in Proceedings of the U.S.–People's Republic of China Workshop on Focused Earthquake Prediction Experiments, *U.S. Geol. Surv. Open File Rep.*, in press, 1994.

Park, S. K., and D. V. Fitterman, Sensitivity of the telluric monitoring array in Parkfield, California, to changes of resistivity, *J. Geophys. Res.*, *95*, 15,557–15,571, 1990.

Parkfield Working Group, Parkfield: First short-term earthquake warning, *Eos Trans. AGU*, *74*, 152–153, 1993.

Poley, C. M., A. G. Lindh, W. H. Bakun, and S. S. Schulz, Temporal changes in microseismicity and creep near Parkfield, California, *Nature*, *327*, 134–137, 1987.

Prescott, W. H., J. L. Davis, and J. L. Svarc, Global Positioning System measurements for crustal deformation: Precision and accuracy, *Science*, *244*, 1337–1340, 1989.

Real, C. R., and B. E. Tucker, Ground motion site effects test area near Parkfield, California, paper presented at 9th World Conference on Earthquake Engineering, Int. Assoc. for Earthquake Eng., Tokyo/Kyoto, Japan, Aug. 2–9, 1988.

Roeloffs, E. A., S. S. Burford, F. S. Riley, and A. W. Records, Hydrologic effects on water level changes associated with episodic fault creep near Parkfield, California, *J. Geophys. Res.*, *94*, 12,387–12,402, 1989.

Ruina, A. L., Slip instability and state variable friction laws, *J. Geophys. Res.*, *88*, 10,359–10,370, 1983.

Sacks, I. S., S. Suyehiro, D. Evertson, and Y. Yamagishi, Sacks-Evertson strain meter, its installation in Japan, and some preliminary results concerning strain steps, *Pap. Meteorol. Geophys.*, *22*, 195–207, 1971.

Sato, M., A. J. Sutton, K. A. McGee, and S. Russell-Robinson, Monitoring of hydrogen along the San Andreas and Calaveras faults in central California in 1980–1984, *J. Geophys. Res.*, *91*, 12,315–12,326, 1986.

Savage, J. C., Criticism of some earthquake forecasts of the National Earthquake Prediction Evaluation Council, *Bull. Seismol. Soc. Am.*, *81*, 862–881, 1991.

Savage, J. C., The Parkfield prediction fallacy, *Bull. Seismol. Soc. Am.*, *83*, 1–6, 1993.

Savage, J. C., and R. O. Burford, Geodetic determination of relative plate motion in central California, *J. Geophys. Res.*, *78*, 832–845, 1973.

Schneider, J. F., N. A. Abrahamson, P. G. Somerville, and J. C. Stepp, Spatial variation of ground motion from EPRI's dense accelerograph array at Parkfield, California, paper presented at 4th National Conference on Earthquake Engineering, Earthquake Eng. Res. Inst., Palm Springs, Calif., May 1990.

Schulz, S. S., Catalog of creep meter measurements in California from 1966 through 1988, *U.S. Geol. Surv. Open File Rep.*, *89-650*, 1989.

Segall, P., and Y. Du, How similar were the 1934 and 1966 Parkfield earthquakes?, *J. Geophys. Res.*, *98*, 4527–4538, 1993.

Segall, P., and R. Harris, Slip deficit on the San Andreas

fault at Parkfield, California, as revealed by inversion of geodetic data, *Science*, *233*, 1409–1413, 1986.

Segall, P., and R. Harris, Earthquake deformation cycle on the San Andreas fault near Parkfield, California, *J. Geophys. Res.*, *92*, 10,511–10,525, 1987.

Segall, P., and D. D. Pollard, Mechanics of discontinuous faults, *J. Geophys. Res.*, *85*, 4337–4350, 1980.

Shearer, C. F., Minutes of the National Earthquake Prediction Evaluation Council, November 16–17, 1984, *U.S. Geol. Surv. Open File Rep.*, *85-201*, 1985*a*.

Shearer, C. F., Minutes of the National Earthquake Prediction Evaluation Council, March 29–30, 1985, *U.S. Geol. Surv. Open File Rep.*, *85-507*, 1985*b*.

Shedlock, K. M., T. M. Brocher, and S. T. Harding, Shallow structure and deformation along the San Andreas fault in Cholame Valley, California, based on high-resolution reflection profiling, *J. Geophys. Res.*, *95*, 5003–5020, 1990.

Sherburne, R. W., Ground shaking and engineering studies on the Parkfield section of the San Andreas fault, *Earthquakes Volcanoes*, *20*, 72–77, 1988.

Sibson, R. H., Stopping of earthquake ruptures at dilational fault jogs, *Nature*, *316*, 248–251, 1985.

Sieh, K. E., Slip along the San Andreas fault associated with the great 1857 earthquake, *Bull. Seismol. Soc. Am.*, *68*, 1421–1428, 1978*a*.

Sieh, K. E., Central California foreshocks of the great 1857 earthquake, *Bull. Seismol. Soc. Am.*, *68*, 1731–1749, 1978*b*.

Sieh, K. E., and R. H. Jahns, Holocene activity of the San Andreas fault at Wallace Creek, California, *Geol. Soc. Am. Bull.*, *95*, 883–896, 1984.

Sieh, K. E., M. Stuiver, and D. Brillinger, A more precise chronology of earthquakes produced by the San Andreas fault in southern California, *J. Geophys. Res.*, *94*, 603–623, 1989.

Silverman, S., C. Mortensen, and M. Johnston, A satellite-based digital data system for low-frequency geophysical data, *Bull. Seismol. Soc. Am.*, *79*, 189–198, 1989.

Simpson, R. W., S. S. Schulz, L. D. Dietz, and R. O. Burford, The response of creeping parts of the San Andreas fault to earthquakes on nearby faults: Two examples, *Pure Appl. Geophys.*, *126*, 665–685, 1988.

Sims, J. D., Geologic map of the San Andreas fault in the Cholame Valley and Cholame Hills quadrangles, San Luis Obispo and Monterey counties, California, *U.S. Geol. Surv. Misc. Field Stud. Map*, *MF-1995*, 1988.

Sims, J. D., Chronology of displacement on the San Andreas fault in central California: Evidence from reversed positions of exotic rock bodies near Parkfield, California, *U.S. Geol. Open File Rep.*, *89-571*, 40 pp., 1989.

Sims, J. D., Geologic map of the San Andreas fault in the Parkfield 7.5-minute quadrangle, Monterey and Fresno counties, California, *U.S. Geol. Surv. Misc. Field Stud. Map*, *MF-2115*, 1990.

Smith, S. W., and M. Wyss, Displacement of the San Andreas fault subsequent to the 1966 Parkfield earthquake, *Bull. Seismol. Soc. Am.*, *58*, 1955–1973, 1968.

Snay, R. A., Enhancing the geodetic resolution of fault slip by introducing prior information, *Manuscr. Geod.*, *14*, 391–403, 1989.

Stuart, W. D., Seismic quiescence at Parkfield due to detachment faulting, *Nature*, *349*, 58–61, 1991.

Stuart, W. D., R. J. Archuleta, and A. G. Lindh, Forecast model for moderate earthquakes near Parkfield, California, *J. Geophys. Res.*, *90*, 592–604, 1985.

Sylvester, A. G., Nearfield geodetic investigations of crustal movements, southern California, National Earthquake Hazard Reduction Program, Final Technical Report, 1988–1990, U.S. Dep. of Inter.-U.S. Geol. Surv. grant 14-08-0001-G1690, 508 pp., Univ. of Calif., Santa Barbara, 1991.

Thatcher, W., Systematic inversion of geodetic data in central California, *J. Geophys. Res.*, *84*, 2283–2295, 1979.

Thatcher, W., and P. Segall, Reid's hypothesis, the time-predictable model, and the Parkfield earthquake (abstract), *Eos Trans. AGU*, *71*, 1473, 1990.

Toppozada, T. R., Parkfield earthquake history (abstract), *Eos Trans. AGU*, *73*(43), Fall Meeting suppl., 406, 1992.

Toppozada, T. R., C. Hallstrom, and D. Ransom, $M \geq 5.5$ earthquakes within 100 km of Parkfield, California, *Seismol. Res. Lett.*, *61*, 42, 1990.

Tsai, Y.-B., and K. Aki, Simultaneous determination of the seismic moment and attenuation of seismic surface waves, *Bull. Seismol. Soc. Am.*, *59*, 275–287, 1969.

Tullis, T. E., and W. D. Stuart, Premonitory changes prior to a model Parkfield earthquake (abstract), *Eos Trans. AGU*, *73*(43), Fall Meeting suppl., 397, 1992.

Tullis, T. E., W. D. Stuart, and R. W. Simpson, Instability model for Parkfield earthquakes, including the effect of New Idria, Coalinga, and Kettleman Hills events (abstract), *Eos Trans. AGU*, *71*, 1632, 1990.

Wallace, R. E., and T.-L. Teng, Prediction of the Sungpan-Pingwu earthquakes, August, 1976, *Bull. Seismol. Soc. Am.*, *70*, 1199–1223, 1980.

Working Group on California Earthquake Probabilities (WGCEP), Probabilities of large earthquakes occurring n California on the San Andreas fault, *U.S. Geol. Surv. Open File Rep.*, *88-398*, 1988.

Wyss, M., Changes of mean magnitude of Parkfield seismicity: A part of the precursory process?, *Geophys. Res. Lett.*, *17*, 2429–2432, 1990.

Wyss, M., Increased mean depth of earthquakes at Parkfield, *Geophys. Res. Lett.*, *18*, 617–620, 1991.

Wyss, M., P. Bodin, and R. E. Habermann, Seismic quiescence at Parkfield: An independent indication of an imminent earthquake, *Nature*, *345*, 426–428, 1990*a*.

Wyss, M., L. Slater, and R. O. Burford, Decrease in deformation rate as a possible precursor to the next Parkfield earthquake, *Nature*, *345*, 428–431, 1990*b*.

J. Langbein, U.S. Geological Survey, 345 Middlefield Road, MS 977, Menlo Park, CA 94025.

E. Roeloffs, Cascades Volcano Observatory, U.S. Geological Survey, 5400 MacArthur Boulevard, Vancouver, WA 98661. (e-mail: evelynr@io.wr.usgs.gov)